Basin Research (2006) **18**, 521–545, doi: 10.1111/j.1365-2117.2006.00306.x

Late orogenic vertical movements in the Carpathian Bend Zone – seismic constraints on the transition zone from orogen to foredeep

K. A. Leever,*† L. Matenco,*† G. Bertotti,*† S. Cloetingh*† and G. G. Drijkoningen*‡

*Netherlands Centre for Integrated Solid Earth Sciences (ISES), Amsterdam, The Netherlands
†Faculty of Earth and Life Sciences, Vrije Universiteit, Amsterdam, The Netherlands
‡Department of Applied Earth Sciences, Delft University of Technology, The Netherlands

ABSTRACT

Postcollisional tectonic movements in orogens and their adjacent foreland basins related to intraplate stresses and the presence of a remnant slab are likely to induce significant deformations overprinting the existing patterns of nappe emplacement. In the Carpathian Bend Zone, Romania, vertical motions associated with very limited postorogenic intraplate shortening are of similar magnitude as those generally caused by large orogenic deformations. In the Latest Miocene–Pliocene, up to 6 km of postcollisional sediments of remarkably parallel stratification were deposited in a basin extending over a large part of the present-day orogen. The Early Quaternary featured a dramatical change as the orogen was uplifted while subsidence continued in the basin, tilting the basin flank adjacent to the orogen to a vertical position. The remnant slab presently below the Bend zone in Vrancea is the prime mechanism to have driven the Pliocene subsidence. The Quaternary changes and the eastwards migration of the pattern of vertical motions can be explained by large-scale folding, in response to the overall compressive regime that is recorded in the whole Pannonian-Carpathian area.

INTRODUCTION

The development of basins adjacent to mountain chains, referred to as foreland basins or foredeeps, is commonly explained by the flexural isostatic response of the lithosphere to orogenic loading by thrusting (e.g. Beaumont, 1981) and (un)loading due to surface mass redistribution by erosion and sedimentation (e.g. Flemings & Jordan, 1989; Johnson & Beaumont, 1995), which is partly climate controlled (e.g. Schlunegger & Simpson, 2002). Although 'hidden loads' have been inferred where basement deflection is larger than expected from thrust loading only (Royden & Karner, 1984), it is typically assumed that foredeep subsidence is basically controlled by the load of the thrust sheets, and that it ends when shortening ends. Ongoing erosion will then lead to uplift of the belt and the flanks of its foredeeps at a wavelength controlled by the rigidity of the lithosphere.

These scenarios are attractive because of their simplicity. However, their overall validity has recently been questioned by the discovery of significant deviations occurring in natural examples, especially during the last stages of orogeny (e.g. Cloetingh *et al.*, 2004). These anomalies mainly concern the magnitude and timing of vertical movements in the fold-and-thrust belts and adjacent sedimentary basins and their temporal relation with the shortening taking place in the orogen. In this contribution, we differentiate between the orogenic stage and the late orogenic stage. The orogenic stage refers to active collision, associated with major shortening (>100 km), nappe stacking and crustal thickening. In contrast, we define the late-orogenic stage as the subsequent period, postdating the main stages of contraction that features only limited shortening and deformation.

Low-temperature thermochronology and subsidence analysis have documented substantial vertical movements in a late orogenic stage (e.g. Bertotti *et al.*, 2003). In simple cases, these movements consist of a couple of exhumation/uplift in the mountain belt and subsidence in the adjacent basin, often coeval (e.g. Bertotti *et al.*, 2006). In more complex cases, the sign of vertical movements of specific parts of the system may change through time (e.g. Bertotti *et al.*, 2001). These movements cannot be reconciled with the models of foredeep development described above.

The coexistence and importance of (late orogenic) vertical movements are clearly visible in the transition zone connecting the mountain belt with the adjacent basin. In the classical model, foredeeps are wedge-shaped basins thickening towards the orogen where the basement deflection is largest. Sediments are deposited in front of the actively deforming zone and dip towards the orogen. Postorogenic uplift due to erosional unloading may result in a (slight) basinward dip (e.g. the Alps – Cederbom *et al.*, 2004). However, in several cases, the sediments adjacent

Correspondence: K. A. Leever, Netherlands Centre for Integrated Solid Earth Sciences, De Boelelaan 1085, 1081 HV Amsterdam, The Netherlands. Tel. +31 20 598 7278; Fax: +31 20 598 9943; E-mail: karen.leever@falw.vu.nl

to the thrust front have been observed to show a steeply basinward-dipping geometry, too steep to be explained by the classical model. Pre- and syntectonic sediments can arrive at such a basinward dip by tectonic wedging/the formation of a triangle zone (sensu Jones, 1996), whereby the foredeep sediments are separated by a detachment horizon from the underlying tectonic wedge. The best known example is the Alberta Syncline in the Southern Canadian Rocky Mountains (e.g. Spratt & Lawton, 1996). Modelling has shown that the formation of a triangle zone requires a weak detachment horizon and is enhanced by syntectonic sedimentation (Bonini, 2001). In contrast, the western flank of the foredeep adjacent to the SE Carpathian Bend Zone (Romania) features steeply basinward-dipping sediments that largely postdate the main stages of tectonic activity in the wedge. This requires a different mechanism: one that can cause sufficient subsidence to accommodate the deposition of a large pile of postorogenic sediments and subsequently reverse the sign of the vertical motions and exhume and fold them. The tilted sediments of the transition zone represent the geometric link relating movements in the mountains and in the basin and, more specifically, between the uplift of the mountain chain and the basin subsidence.

In this contribution, we present the results of our work on the transition zone connecting the SE segment of the Carpathian belt with its foredeep (Fig. 1), the Focşani Depression. This basin has accommodated more than 10 km of Miocene–Quaternary sediments. Up to 6 km of sediments have accumulated after the end of major contraction

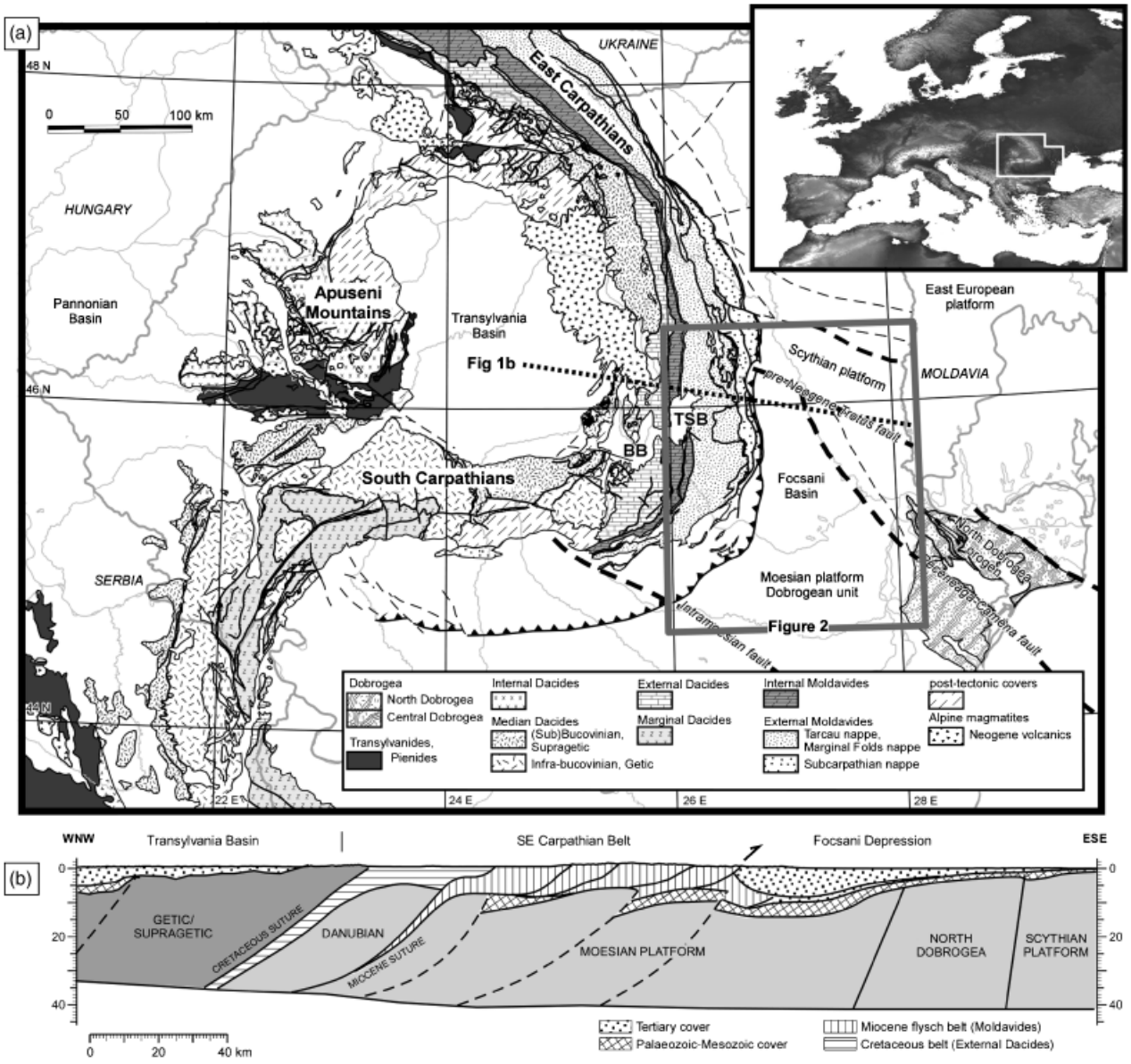

Fig. 1. (a) General location map of the Focşani basin and the adjacent thin-skinned units in the Romanian Carpathians orogenic system (from Săndulescu, 1984, slightly modified with foreland structures from Visarion *et al*., 1988; Răbăgia & Matenco, 1999). BB, Brasov basin; TSB, Tîrgu Secuiesc basin. (b) Simplified crustal scale structural section across the SE Carpathians. Location in Fig. 1a. Modified after Schmid *et al*. (in press).

(Tărăpoancă *et al.*, 2003). On the neighbouring orogenic side, between 2 and 5 km of erosion has taken place in the fold-an-thrust belt during the last 10 Myr (e.g. Sanders *et al.*, 1999; Merten *et al.*, 2005). Quantitative understanding of vertical and horizontal movements in the basins associated with the Carpathians is important also because this orogen is the type locality for models addressing unusual variability in plate kinematics during the late stages of orogeny (e.g., Royden, 1993; Chalot-Prat & Girbacea, 2000; Wortel & Spakman, 2000; Sperner *et al.*, 2001; Gvirtzman, 2002; Cloetingh *et al.*, 2004; Knapp *et al.*, 2005). Different models obviously lead to different interpretations of the large intermediate mantle-depth Vrancea seismicity (e.g. Oncescu & Bonjer, 1997).

The abundance of models is partly the consequence of the paucity of data, especially those able to constrain the geometry of the transition between the Carpathian orogen and the Focşani Depression. As a consequence, the magnitude and timing of vertical movements and tilting in the area are poorly defined. To bridge this gap, the Netherlands Research Centre for Integrated Solid Earth Science (ISES) acquired in 2002 a series of high-resolution seismic lines (lines A, C, D, Fig. 2), aiming at a detailed reconstruction of the subsurface continuation of the exposed stratigraphy. Two of these seismic lines, along the Putna and Rîmnicu Sărat valleys, display with high accuracy the structure of the western and inner flank of the Focşani Basin (Figs 2 and 3). The third one targets Quaternary deformations taking place further eastwards and within the foreland platform units. After a presentation of the seismic lines, we will expand our analysis across the orogen to capture the entire wavelength of the vertical motions, going from the Transylvania Basin in the west to the Carpathian foreland in the east. Finally, we propose a model for the late orogenic movements in the area.

REGIONAL GEOLOGY AND TECTONIC SETTING: ROMANIAN CARPATHIANS AND FORELAND

The Carpathians are a highly arcuate orogen formed in response to the Alpine collision between the upper plate(s) (Tisza-Dacia and Alcapa, senso Bala, 1986) and a relatively stable European foreland in a lower plate position (e.g. Dumitrescu & Săndulescu, 1970; Burchfiel, 1976; Royden, 1988; Săndulescu, 1988; Csontos, 1995; Krzywiec, 2001 and references therein; Fig. 1). The Alpine tectonic history of the Romanian part of the Carpathians may be briefly summarized (Săndulescu, 1988) into a Mesozoic period of extension associated with the formation of two oceanic basins (Transylvanides and outer Dacidian trough) and their subsequent polyphase closure starting in the Cretaceous and culminating with the Sarmatian continental collision in the external domain (10–11 Ma). This collision reflects the stage when the nonthinned lower plate starts to underplate during convergence, leading to thrusting on top of the undeformed foreland (regarding the timing, see Dumitrescu & Săndulescu, 1970). From the end of the Sarmatian onwards, this collision led to the locking and a generalized exhumation of the mountain belt (e.g. Sanders *et al.*, 1999). At the same time, the main hinterland basin, i.e. Transylvania, was uplifted and eroded (e.g. Ciupagea *et al.*, 1970; Ciulavu *et al.*, 2002).

In front of the Carpathians, a foredeep basin developed with substantial along-strike variations in width and thickness. Maximum subsidence rates in the entire foredeep took place in Sarmatian time (Fig. 4), coeval with and related to collision of the East and South Carpathians with their forelands (Matenco *et al.*, 2003). The largest sediment thicknesses are observed in the Focşani Depression (Figs 1–3; e.g. Matenco *et al.*, 2003; Tărăpoancă *et al.*, 2003), which has consistently been the most subsiding area throughout the Miocene to Present (Bertotti *et al.*, 2003). Classical geodetic levelling (e.g. Popescu & Dragoescu, 1986) and preliminary GPS (e.g. Van der Hoeven *et al.*, 2005) studies have shown that the Focşani Basin is still rapidly subsiding with up to 3 mm year^{-1}. Meanwhile, the neighbouring orogenic wedge experiences a rapid uplift of up to 2–3 mm year^{-1}.

The bend zone

The Carpathian Bend Zone is the transition between the N–S-striking East Carpathian belt and the E–W-trending South Carpathian orogen (Fig. 1). The orogenic nappe pile in the study area (e.g. Săndulescu, 1988) is composed of a stack of basement and Mesozoic cover nappes (Middle Dacides), tectonically overlying the thin-skinned flysch nappes deformed during the closure of the Outer Dacidian trough. In the Bend Zone, the main detachment, i.e. the Pericarpathian thrust front, is buried below Upper Miocene – Quaternary sediments (e.g. Dicea, 1995; Matenco & Bertotti, 2000; Fig. 1).

The Bend Zone has a number of distinctive features. It is the site of the most recent tectonic activity of the entire Carpathians arc. Following the early Late Miocene (Sarmatian) collision and after a Latest Miocene–Early Pliocene period of relative thrusting quiescence, contraction in the Bend zone apparently restarted in Late Pliocene–Quaternary times (Wallachian phase, senso Săndulescu, 1988), with <10 km shortening (Matenco & Bertotti, 2000). This led to the formation of small-scale out-of-sequence thrusts with roughly SW-ward vergence (see also Hippolyte & Săndulescu, 1996; Morley, 1996; Zweigel *et al.*, 1998). This deformation is coeval with the regional Pliocene–Quaternary inversion, which affected the Pannonian (e.g. Horváth, 1993; Bada *et al.*, 1999; Fodor *et al.*, 1999, 2005) and Transylvania (e.g. Ciulavu *et al.*, 2002) basins.

A second unusual feature of the Bend Zone is its Pliocene–Quaternary denudation (up to 5 km of erosion), largely postdating other East and South Carpathians areas, where major exhumation (>5 km) took place during Middle-late Miocene (Badenian–Sarmatian) times (Sanders *et al.*, 1999).

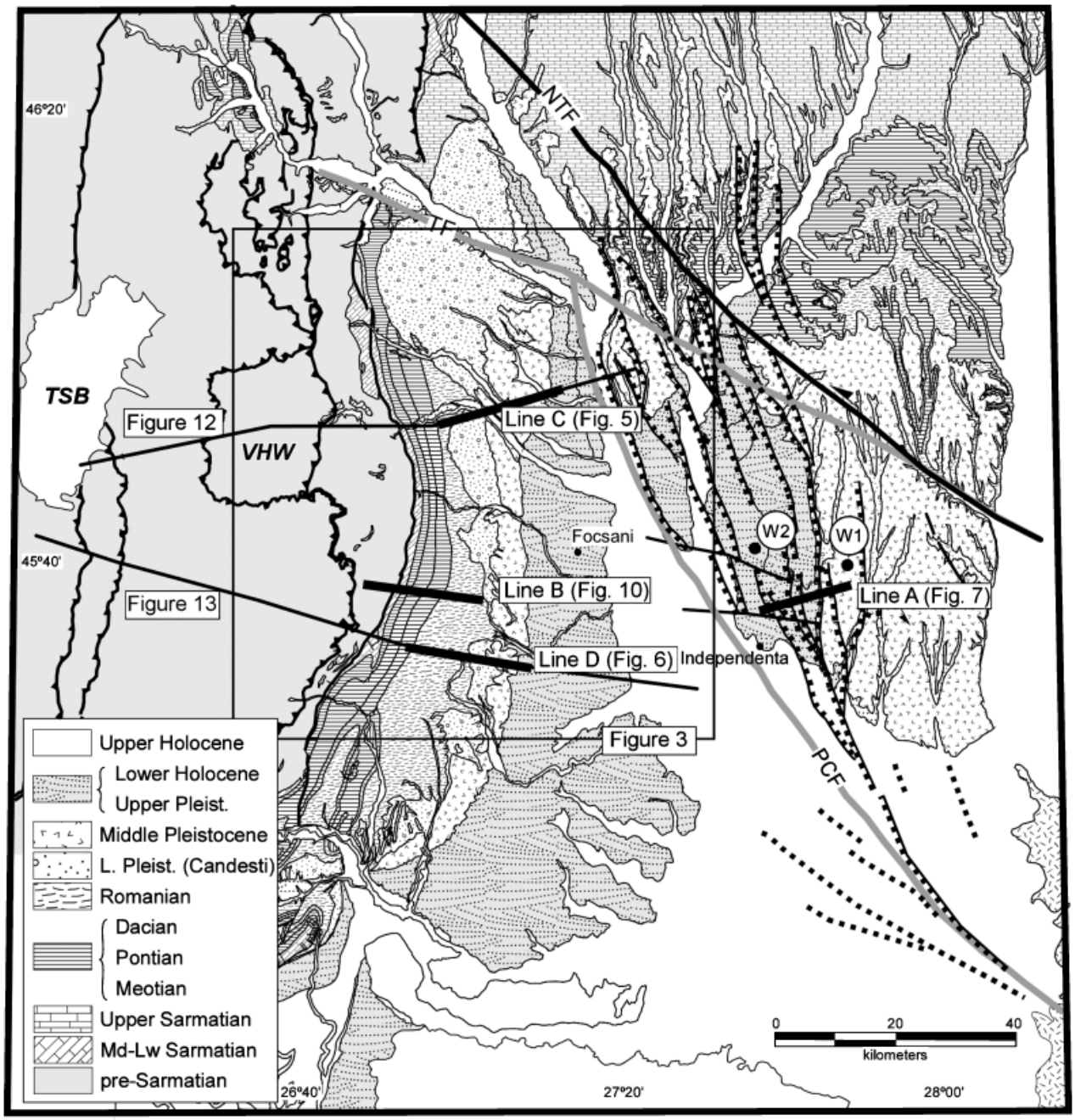

Fig. 2. Detailed geological map of the SE Carpathians foreland with the location of depth data used in the present study (simplified from 1:200 000 maps published by the Geological Institute of Romania). Bold black lines indicate the shallow seismic lines (lines C, D, A) and the industry line (line B), displayed in Figs 5–7 and 10, respectively. Triangular toothed lines: main (nappe bounding) thrusts in the orogen; Block-toothed lines: Sarmatian, recent normal faults; VHW, Vrancea half-window; TSB, Tirgu Secuiesc Basin; PCF, Peceneaga–Camena fault; TF, Trotus fault; W1, W2, location of the wells used for the depth conversion of the Independenţa line (Fig. 7).

The Bend Zone is still seismically active. Whereas seismicity is minor in other segments of the Carpathians chain, the SE part of the belt releases the largest strain accumulation in continental Europe (e.g. Wenzel *et al.*, 1999). The high earthquake recurrencies (25 years for Mw >7 and 50 years for Mw >7.4) are limited to a spatially restricted, $40 \times 80 \times 200$ km, seismogenic volume (Oncescu & Bonjer, 1997) located at $\sim$100 km SE of the expected position of the plate boundary (e.g. Radulian *et al.*, 2000).

The Carpathian foreland and the Focşani Depression

The undeformed foreland of the Carpathians is composed of an amalgamation of three major units with different geometries and characteristics. They represent cratonic continental platforms (senso Twiss & Moores, 1992) with Precambrian crystalline rocks and a Palaeozoic–Mesozoic sedimentary cover. These units (Fig. 1) comprise the

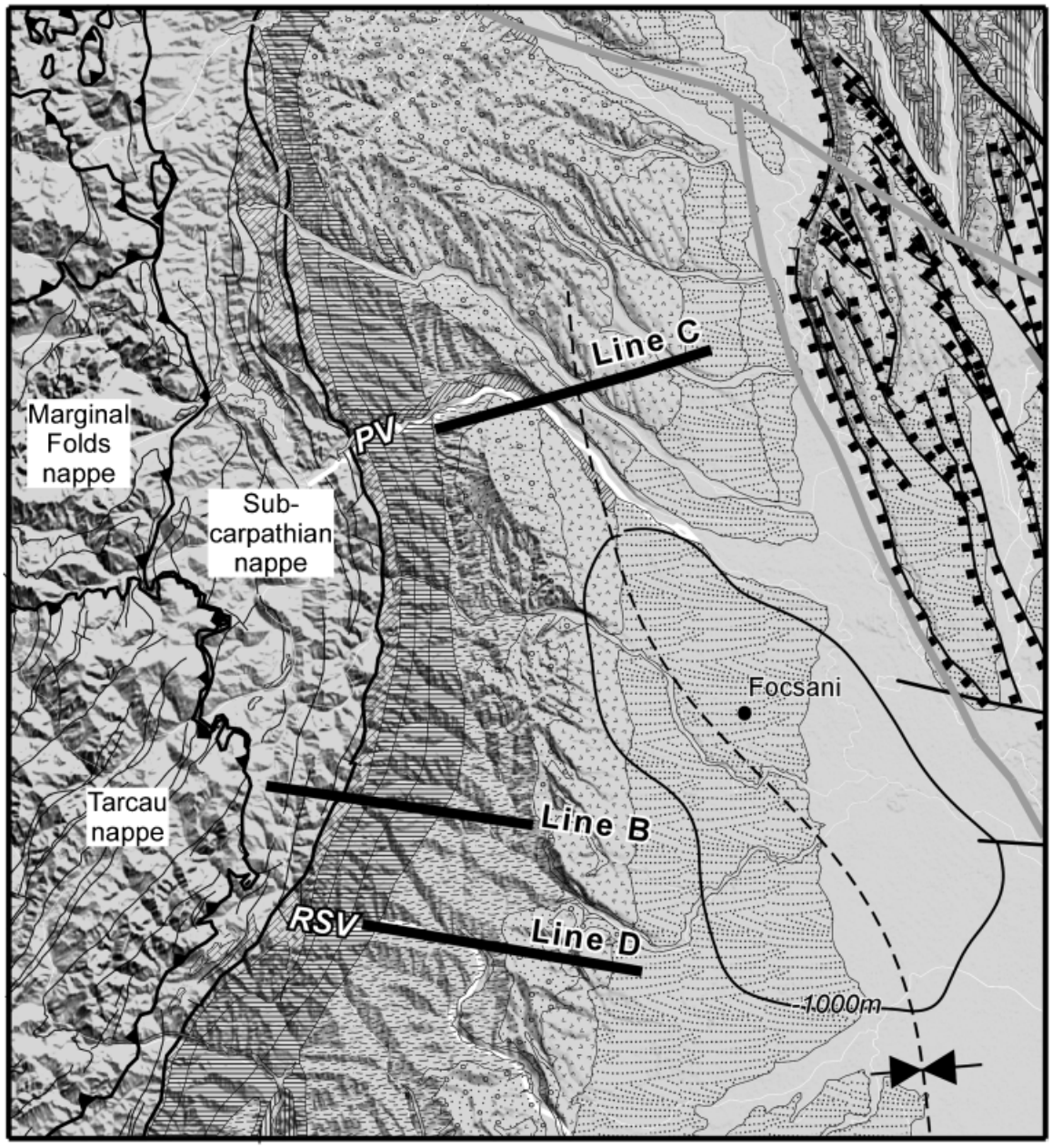

Fig. 3. Geological map draped over a 90-m resolution DEM (SRTM, Rabus *et al*., 2003) along the western flank of the Focşani basin. Lines C, D and B represent locations of the seismic lines in Figs 5, 6 and 10. Legend for geological units as in Fig. 2. Note the high elevation of the Pliocene–Quaternary strata and their deep burial in the frontal foredeep. Note also the location of the Focşani basin Pliocene depocentre roughly in the frontal part of line B. PV, Putna valley; RSV, Rîmnicu Sărat valley. The thick black line in the centre of the basin represents the contour of − 1000 m of the base Quaternary horizon, whereas the dashed line is the Focşani basin axis (after Matenco *et al*., in press).

East-European, Scythian and Moesian platforms. A fourth unit is North Dobrogea, which contains remains of a Hercynian orogen, which was subsequently subjected to Mesozoic rifting and inversion (e.g. Seghedi, 2001).

The part of the foreland adjacent to the Carpathian Bend Zone, corresponding to the Moesian Platform, has been the site of major subsidence since the Middle Miocene (e.g., Dicea, 1995; Răbăgia & Matenco, 1999). Foredeep sediments are almost entirely shallow lacustrine to near-shoreline continental deposits, deposited in an Eastern Paratethys domain (Dacic Basin senso Jipa, 1997), spatially separated at various time levels from the main Tethyan realm (e.g. Kovač *et al*., 1999; Rögl, 1999). Extreme subsidence values are observed in a restricted area of the Dacic Basin, $\sim 30 \times 50$ km in surface, known as the Focşani Depression. Here, up to 13 km of sediments were deposited during Neogene-Quaternary times (Tărăpoancă *et al*., 2003).

Strong subsidence in Middle to Late Badenian times (Middle Miocene) postdates the regional deposition of evapourites and accommodates the deposition of thick clastics. Normal faults (Tărăpoancă *et al*., 2003) indicate a

period of limited NNE–SSW extension. Coeval with collision, thick clastic sediments are deposited during the Sarmatian, associated with further normal faulting related to flexural bending of the underthrust foreland plate (Tărăpoancă *et al.*, 2003; Leever *et al.*, 2006).

During the late orogenic stage (i.e. post-Late Sarmatian), foreland subsidence continued only in the Moesian block, with particularly high values in the Focşani Basin. Upper Miocene (Meotian–Pontian) sediments are shallowwater clastics and are overlain by Pliocene prograding deltaic bodies that filled the Dacic Basin, except for the Focşani area (e.g. Jipa, 1997). Here, subsidence accelerated during the Pliocene–Quaternary, whereas its western part was progressively uplifted, imposing a shift of the depocentre towards SE (Matenco *et al.*, 2003; Tărăpoancă *et al.*, 2003).

The Focşani Basin flanks

The western Focşani Basin flank, i.e. its transition to the Carpathian thrust belt, is characterized by a 5–6 km thick sequence of Late Miocene–Pliocene shallow lacustrine sediments, dipping towards the east (Fig. 3). The western limit of the succession is a poorly exposed fault zone that forms the contact with the Subcarpathian nappe. The geometry and kinematics of this fault are ambiguous: surface structural observations by the authors indicate an east vergent thrust, whereas existing interpretations of the structure at depth suggest a large scale backthrust, forming a triangle zone rooted in the buried Pericarpathian thrust (Roure *et al.*, 1993; Matenco & Bertotti, 2000).

The westernmost foredeep sediments are Upper Sarmatian–Meotian sandy turbidites changing upsection to finer-grained Pontian–Lower Dacian turbidites and eventually to Upper Dacian–Romanian shallow lacustrine deposits (Marinescu *et al.*, 1981; Fig. 4) The (sub)vertical dips in the Sarmatian deposits gradually decrease to 15° in the upper Pliocene strata. The Miocene to Pliocene succession is overlain by massive gravels (Cîndeşti gravels) deposited by sheet flows (senso Einsele, 2000) in a shallow lacustrine to alluvial environment and dated as Uppermost Pliocene(?)–Lower Pleistocene. The gravels dip ~5–10° to the E and display an unconformable contact with the underlying Pliocene strata north of the Putna valley (Figs 2 and 3). The Cîndeşti gravels presently crop out at elevations of up to 1 km, and are unconformably covered by several levels of Middle Pleistocene–Holocene loess and alluvial deposits, locally dipping up to 2–3° (Necea *et al.*, 2005).

The eastern flank of the Focşani Depression is very different from the western one and characterized by eastward shallowing of the basin floor overprinted by a regional system of presently active normal faults. This system is spatially juxtaposed with the Peceneaga–Camena fault (Fig. 2, Matenco *et al.*, in press), a deep crustal fracture with a Moho offset of ~5 km (Rădulescu *et al.*, 1976) separating the Moesian platform from the Neogene buried part of the North Dobrogea orogen (Visarion *et al.*, 1988).

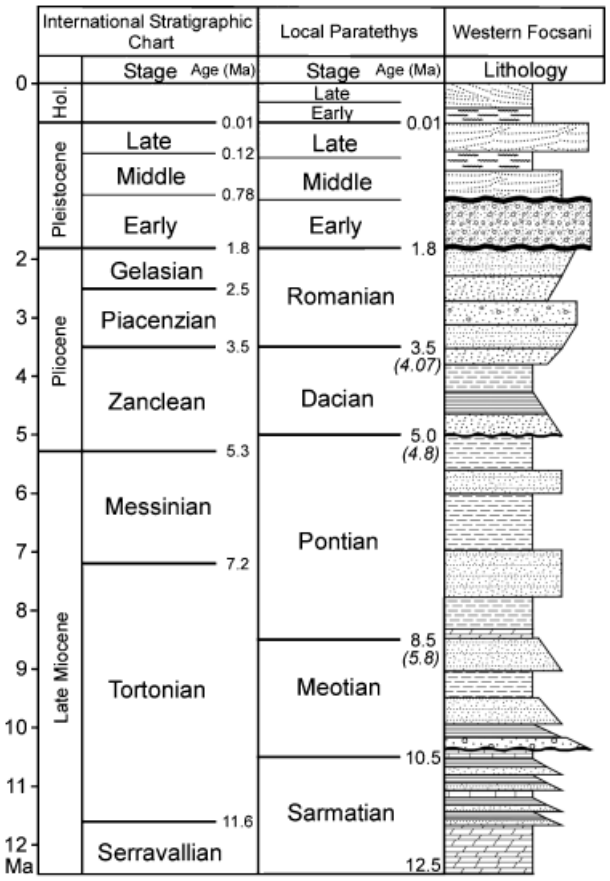

Fig. 4. Lithostratigraphic column of the exposed Upper Miocene–Quaternary sediments on the western flank of the Focşani basin and correlation between the standard Tethys and Eastern Paratethys ages used in the present study (after Rögl, 1999). Ages in italics are the absolute values obtained by magnetostratigraphy (Vasiliev *et al.*, 2004, 2005).

ACQUISITION, PROCESSING AND DEPTH CONVERSION OF THE SHALLOW SEISMIC LINES

In this section, we present the three high-resolution shallow seismic lines that were acquired in 2002 in the framework of the ISES project CARFOR. Two of the seismic lines (location in Figs 2 and 3) are located on the western flank of the Focşani Depression; the third one traverses the eastern flank of the basin and the Peceneaga–Camena fault system.

Acquisition and processing, quality of the sections

The sections on the western basin flank cross the Carpathian foothills along the Putna (line C, Fig. 5) and Rîmnicu Sărat valleys (line D, Fig. 6), perpendicular to the structural grain of the late orogenic foredeep sediments. The Putna and Rîmnicu Sărat valleys are easily accessible and provide an almost continuous succession of outcrops necessary for surface calibration of the structural study and for age control provided by the palaeomagnetic

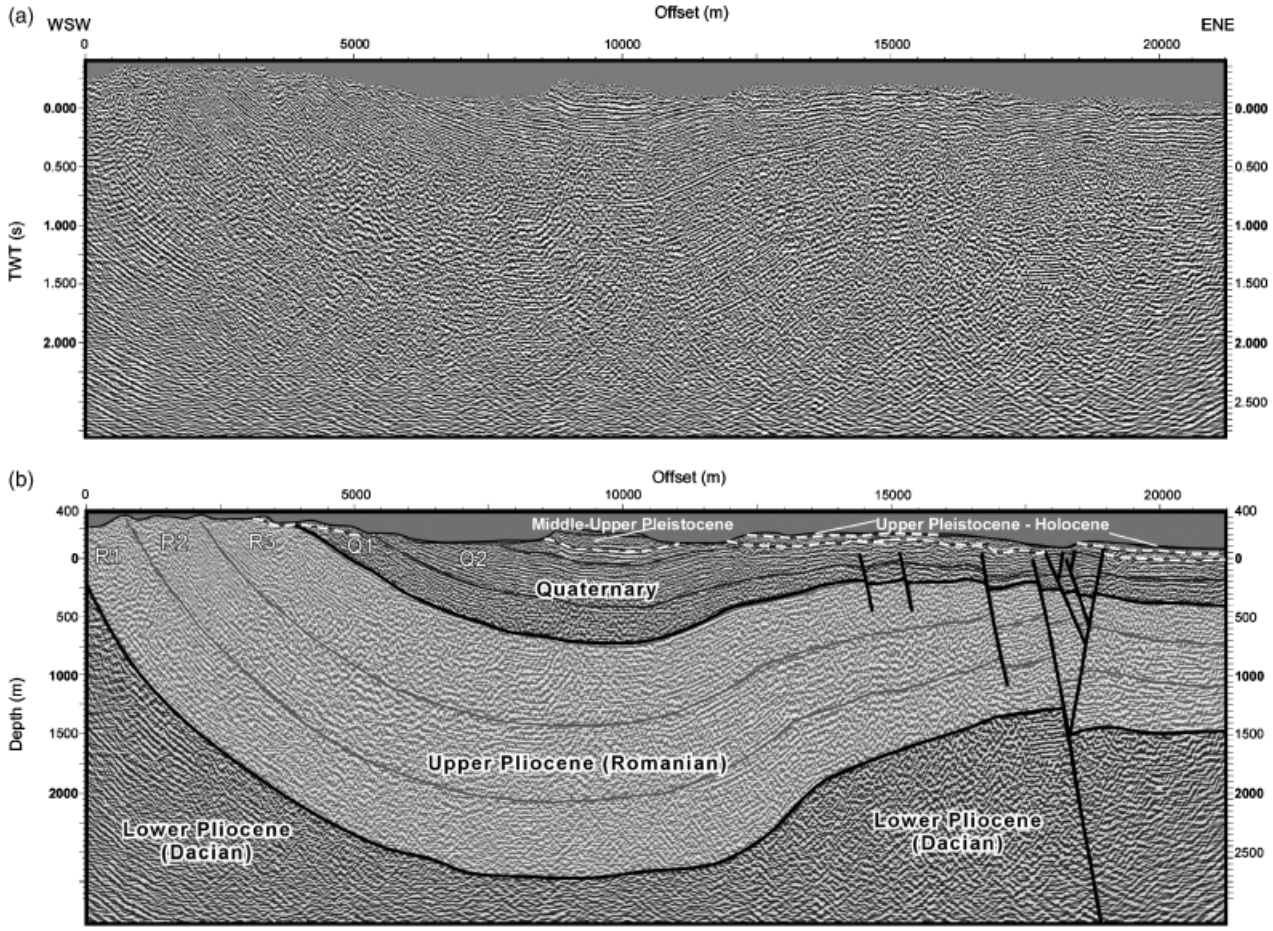

Fig. 5. High-resolution shallow seismic line C on the western flank of Focşani Basin along Putna valley (location in Fig. 3). (a) Interpreted seismic section, vertical scale in seconds two-way travel time. (b) Depth-converted seismic line using velocity model 1 (Fig. 8a).

sampling (Vasiliev *et al*., 2004). In the western part of the profiles, acquisition was stopped where dips exceeded 40–50°. The elevation difference along the sections is approximately 400 m, with forested and accentuated terrain in the western part of the sections (Fig. 3). The third seismic line, located near the village of Independenţa (Fig. 2), traverses the eastern flank of the Focşani Basin and the Peceneaga–Camena fault system (line A, Fig. 7). The position of this line was selected on the basis of available oil industry seismic lines, in an area where deformation concentrates on a narrower zone, i.e. along fewer faults with higher offsets.

The seismic lines were acquired and processed by SC Prospectiunii SA (Bucharest, Romania). Acquisition was designed such as to enhance the vertical and horizontal resolution by very close spacing of geophones and shotpoints, and using a high-frequency pulse (Table 1). An array of 12 geophones was used at each receiver location, 160 live channels being organized in a split spread with a width of 800 m. Processing of the seismic lines was performed in a standardized way, as is indicated in Table 2.

The images obtained from our high-resolution seismic lines are generally of high quality (Figs 5–7) with clear reflectors visible within and well below the target depth of 1 s two-way travel time (TWT). The vertical resolution in the upper part of the sections is *ca*. 20 m. At 2-s TWT this is reduced to 40 m. Attenuation of the high-frequency signal is generally observed at depth. In the lower part of the western sections (C and D, Figs 5a and 6a), the low signal-to-noise ratio (SNR) is ascribed to the steep ($>40^\circ$) dip of the strata. Here, the sections are characterized by low-amplitude, cross-cutting events that steeply dip in both directions, a side effect of processing (migration). At some locations, the signal is disturbed by (sub)vertical 'noise shadows' that penetrate the entire section, generally corresponding to steep topographic features (e.g. at 13.8 km in section C, Fig. 5). A short wavelength ($\sim$15 ms) signal is observed down to 1 s TWT and $\sim$30 ms below in the areas not affected by the noise shadows. In the Rîmnicu Sărat section (Fig. 6), low- to intermediate-amplitude reflectors are very continuous (over a distance of >4 km), with regularly occurring ($\sim$0.25 s) high-amplitude signals. A high-amplitude, low-frequency signal occurs in the upper 0.5 s in the extreme east of the section. Also the Putna line (Fig. 5) is characterized by highly continuous reflectors. Only between 14.5 and 17 km, an irregular, low-frequency, low-continuity signal is observed in the upper 0.5 s, possibly linked to faulting, the zone below being dominated by

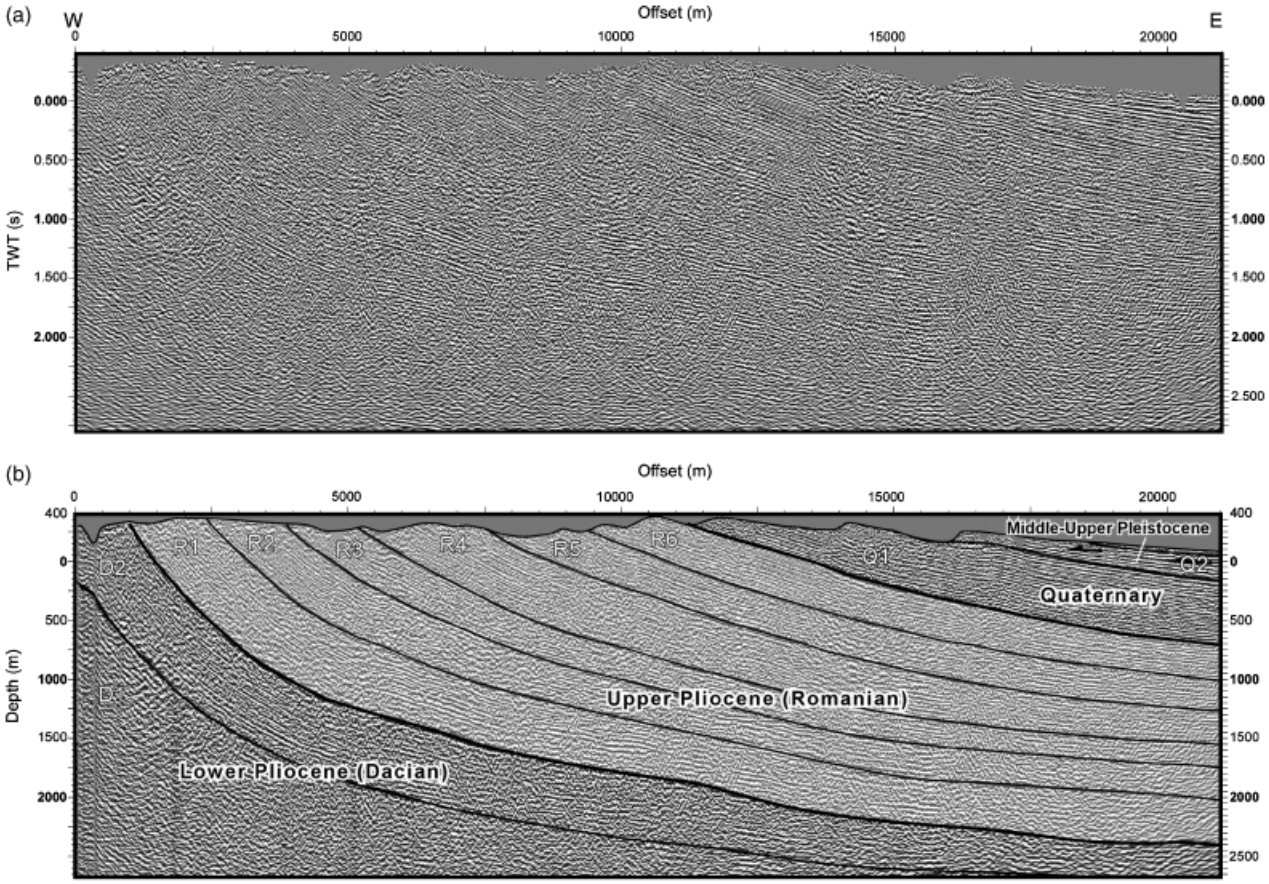

Fig. 6. High-resolution shallow seismic line D on the western flank of Focşani Basin along Rîmnicu Sărat valley (location in Fig. 3). (a) Interpreted seismic section, vertical scale in seconds two-way travel time. (b) Depth-converted seismic line using velocity model 1 (Fig. 8a).

noise. The Independenţa line (Fig. 7) has a good penetration up to 2.5 s TWT. Noise dominates below this depth, preventing the accurate definition of the contact between the foredeep succession and the pre-Neogene basement. In the target interval of < 1 s area, the section shows detailed strata truncations, whereas the stratigraphy is constrained by well ties and corroborated by the seismic facies. This allows for a detailed kinematic reconstruction, not available so far in the published seismic lines (e.g. Tărăpoancă *et al.*, 2003). Fault diffractions are often observed along the section, whereas the high frequencies are attenuated below 1.5 s.

Depth conversion

We performed an accurate time-depth conversion of the seismic lines on the western flank of the Focşani Depression (Lines D and C, Figs 5 and 6) in order to detect changes in thicknesses, that are critical for positioning the Focşani Basin depocentres at various geological time intervals. In the absence of direct time-depth constraints from neighbouring wells, depth conversion is based on velocity modelling (Etris *et al.*, 2001). The results of three different velocity models are discussed below. For line A (Fig. 7), we used time–depth relationships derived from two neighbouring wells (wells W1 and W2, Fig. 2) from which mean interval velocities for the main stratigraphic horizons were extracted.

Three different velocity models (Fig. 8a) were tested for depth-converting sections C and D. Model 1 is based on interval velocities derived from processing (Fig. 8b and c), Model 2 uses velocities from regional velocity maps (Fig. 8b and c; Tărăpoancă *et al.*, 2003) and Model 3 applies a linearly downwards increasing velocity. Sensitivity analysis by comparing the dips of the depth-converted sections with field measurements showed that depth conversion according to Model 1 is most reliable.

Model 1

For this model, velocities were obtained from processing. Processing velocities, however, are imaging velocities, used in stacking and migration for proper lateral positioning of the horizons (Etris *et al.*, 2001). They are not, strictly speaking, the vertical velocities required for proper depth conversion and therefore they must be ultimately calibrated with field or well data. Because these velocities also contain a horizontal component, the values tend to be overestimated (by up to 30% for shales) due to anisotropy. Depth conversion requires interval velocities, which were

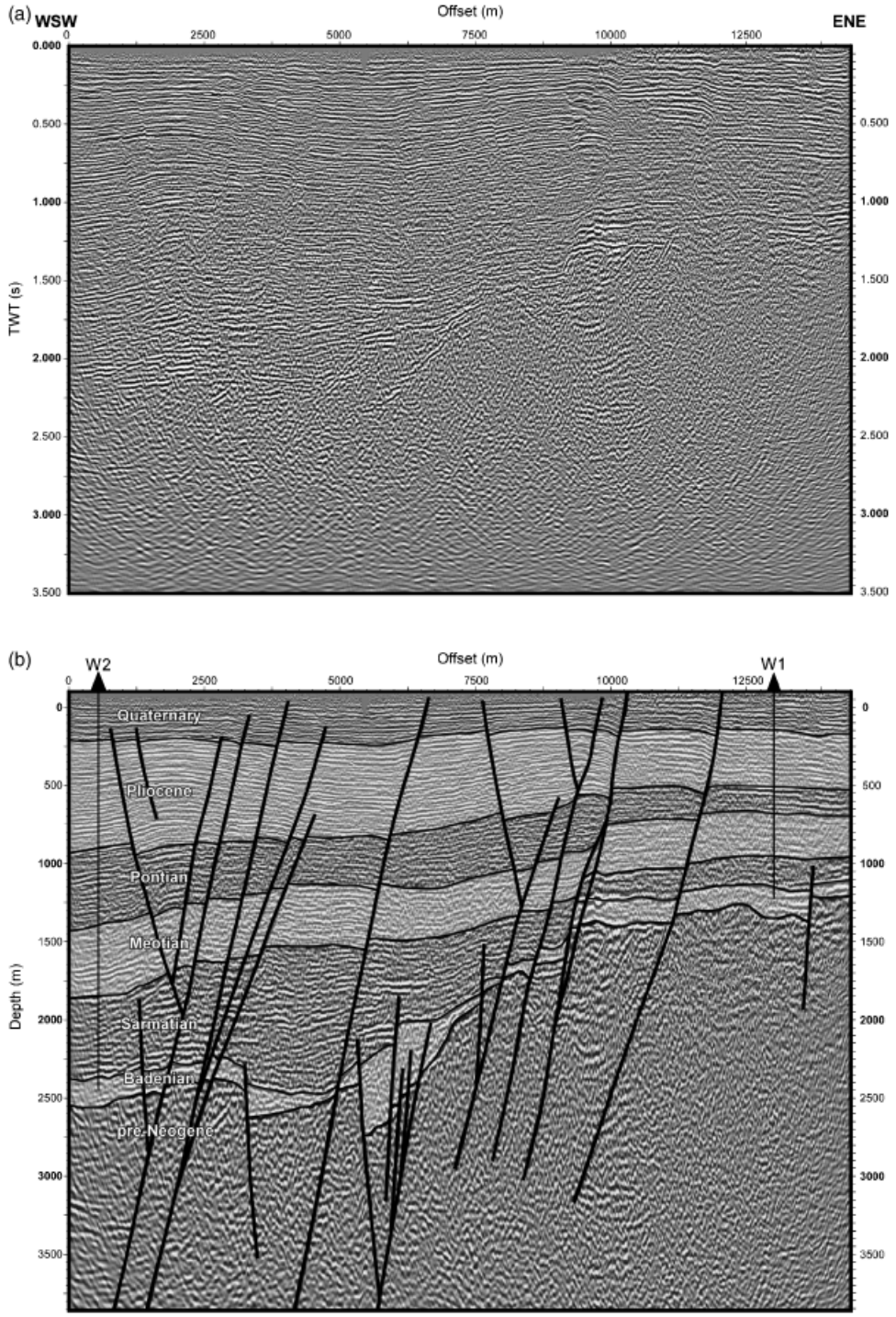

Fig. 7. High-resolution shallow seismic line A in the SE part of the Focşani basin crossing the contact between the Moesian platform and the North Dobrogea Orogen across the Peceneaga–Camena fault system (location in Fig. 2) (a) Interpreted seismic line, vertical scale in seconds two-way travel time. (b) Depth-converted seismic line showing projected positions of wells W1 and W2 (Fig. 2).

derived from root-mean-square (RMS) velocities over horizontal intervals of 300 ms. At depth, the effects of the poorly consolidated near-surface sediments as present on the RMS velocities cancel out, because for the determination of interval velocities, differences of RMS velocities are taken from different depth levels. With the acquisition spread of 800 m used for our sections, the processing velocity information is reliable down to approximately 800 m. The velocities obtained from the upper interval (0 to ~300 ms, Fig. 8b and c) are compatible with the 'standard' values in Table 3, while the two deeper intervals (~300 to ~900 ms) produce much higher values. The velocities show a trend of eastwards-decreasing values, which is more gradual for section D (Rîmnicu Sărat) than for sec-

Table 1. Acquisition parameters of the shallow seismic lines (Figs 5–7)

Spacing	Shot points at 20 m receivers at 5 m
Source	0.1 kg of dynamite at 2 m depth
Receiver	Array of 12 geophones, 10 Hz
Live channels	160
Sample rate	1 ms
Record length	4 s

Table 2. Processing sequence of the shallow seismic lines (Figs 5–7)

Primary seismic field data loading and input of all relevant information
Trace editing (noisy or dead channels, reverse polarity, etc.)
Inline geometry header load
First break picking and the editing of their values in the database
Refraction statics with DRM method and apply refraction statics in all trace headers
F–K filtering and/or band pass filtering (if necessary, depending upon data quality)
Surface consistent deconvolution
Velocity analysis and residual static corrections in two passes at least
DMO
CDP/ensemble Stack
Band pass Filter
F–X deconvolution
FD time migration
Band pass filter
F–X deconvolution
Normalization (AGC) applied any time when necessary to enhance data quality or when requested by some processing operation

tion C (Putna). This trend coincides with the properties of the sediments exposed along the seismic sections: these change from well-consolidated massive calcareous sandstones in the west to poorly consolidated Romanian sands and Quaternary gravels/loess in the east. Keeping in mind the reservations about the application of processing velocities for depth conversion, the velocities that we used (Table 4) are therefore based on those in the upper interval, extrapolated downward along the stratigraphic intervals.

Model 2

Along horizon maps based on the interpretation of seismic profiles through the entire Focşani Basin and adjacent regions, velocities have been calculated from 60 wells for five Neogene–Quaternary intervals (Tărăpoancă *et al*., 2003). Of these, we used the Meotian and Pontian maps. The maps turned out to be rather coarse for our high-resolution targets, the closest well with time-depth constraints being at a distance of 20 km. Because of lack of seismic data on the western flank of the Focşani Depression when these maps were generated (Tărăpoancă *et al*., 2003), the depths

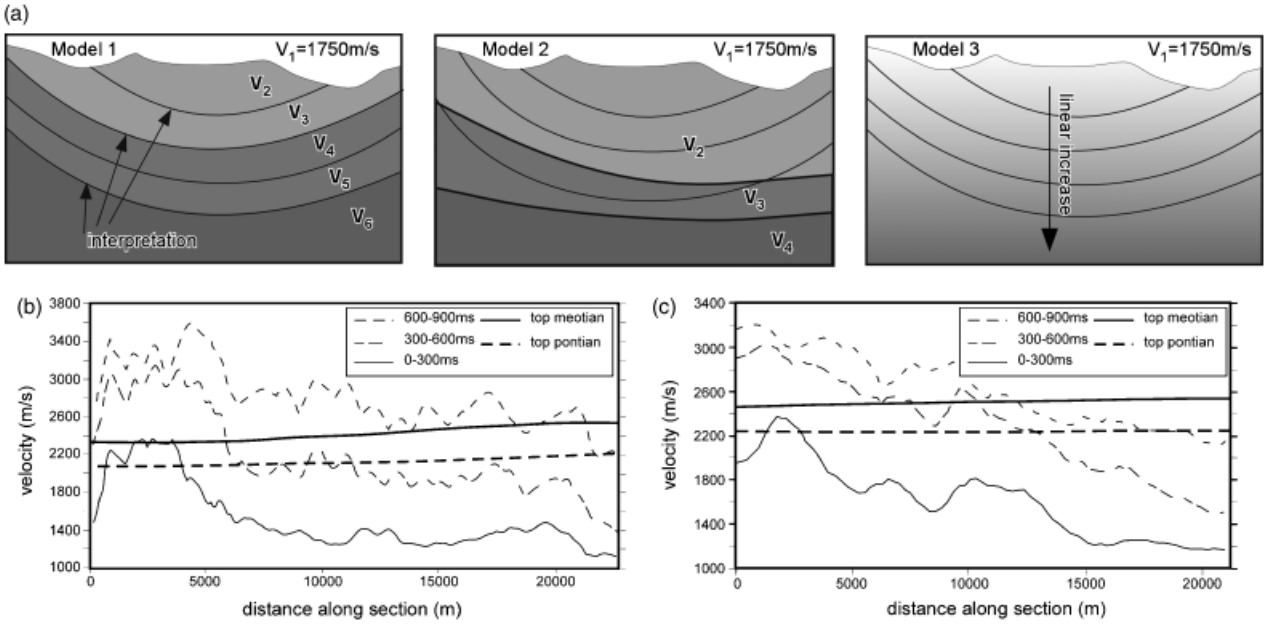

Fig. 8. (a) Velocity models tested for depth conversion. Model 1: each interpreted interval is assigned a velocity based on processing velocities; Model 2: well-derived velocities along regional horizon maps where V2, V3, V4 are velocities for Pliocene–Quaternary, Pontian and Meotian, respectively; Model 3: velocity increases linearly with depth. Different velocities indicated by shades of grey: darker colour represents higher velocity. (b)Velocity data along Putna and (c) along Rîmnicu Sărat sections. Thin lines: interval velocities derived from processing (used in Model 1, Fig. 8a). Note eastward decrease for all intervals. Heavy lines: velocities derived from regional velocity maps (Model 2, a).

Table 3. Standard seismic velocities (compressional wave velocities) in km/s (from Kearey *et al.*, 2002)

Unconsolidated materials		Sedimentary rocks	
Sand (dry)	0.2–1.0	Sandstones	2.0–6.0
Sand (water-saturated)	1.5–2.0	Tertiary sandstone	2.0–2.5
Clay	1.0–2.5		

Table 4. Input velocities (in m/s) used for depth conversion, derived from processing velocities (Model 1) and regional velocity maps (after Tărăpoancă *et al.*, 2003; Model 2). The names of the intervals shown in the left column correspond to the intervals in Figs 5 and 6

Interval	Putna section, V (m/s)		Rimnicu Sarat section, V (m/s)	
	Model 1	Model 2	Model 1	Model 2
Topo	1750	1750	1750	1750
Q-Rm-Dc	–	2150	–	2230
Pontian	–	2400	–	2500
Meotian	–	2650	–	–
Q3	–	–	1500	–
Q2	–	–	1600	–
Q1	1750	–	1700	–
R6	1800	–	1800	–
R5	1900	–	1900	–
R4	2100	–	2000	–
R3	2350	–	2100	–
R2	2400	–	2200	–
R1	2400	–	2300	–
D2	–	–	2400	–
D1	2500	–	2500	–

of the Meotian and Pontian horizons are underestimated with respect to our sections. These horizons constrain the intervals to which the velocities (Table 4) for Pliocene–Quaternary, Pontian and Meotian are attributed. Figure 8b and c shows that the velocities obtained for both the Putna and the Rîmnicu Sărat section are relatively constant, corresponding to realistic values for Tertiary sandstone (Table 3).

Model 3

As seismic velocities will generally increase with depth due to compaction, this velocity model assumes simply a linearly downwards-increasing velocity, $v_z = v_0 + kz$, where z is the depth in m, v_0 is the velocity at $z = 0$ (1750 m s^{-1}), and k is the rate of change in velocity with depth ($k = 0.5$). Integration gives the depth-time relation: $z = v_0 \times (e^{kt}–1)/k$, where t is the one-way travel time in seconds.

Comparing the dips from the depth-converted sections with field measurements, Model 3 shows the largest deviation for both sections, up to 8–9° in the western part of the sections. This is due to the fact that the eastwards-younging trend of the sediments was not taken into account in this model. Models 1 and 2 give very similar results for line C (Putna), showing a deviation of up to 5° in the eastern part of the section. For the Rîmnicu Sărat section (line D), the best results are obtained by Model 1: the dips of the depth-converted section deviate by only 2° from the field data. The depth-converted sections in Figs 5b and 6b are thus obtained from the velocities in Model 1 (Table 4).

RESULTS OF SEISMIC INTERPRETATION

Interpretation of the depth-converted shallow seismic lines (Figs 5 and 6), together with a third line traversing the contact between basin and thrust belt just to the north of the Rîmnicu Sărat valley (Fig. 9, locations in Fig. 2), allowed us to constrain the kinematics of the western flank of the Focşani Basin and to define the nature of the contact between the foredeep sediments and the thrust wedge.

Geometry of the folded Pliocene–Quaternary strata on the western flank of the Focşani Basin

For the interpretation of the shallow seismic lines (Figs 5 and 6) we projected the formation boundaries derived from the 1 : 200 000 geological maps to depth (Figs 2 and 3).

The first-order structure imaged along the Putna section is an asymmetric syncline (Fig. 5b). Reflectors are steep and E-ward dipping in the W, become horizontal, subsequently acquire a gentle dip to the W and regain their subhorizontal position towards the eastern termination of the line. Reflectors are continuous over large distances (< 4 km), with mostly subparallel strata with no lateral terminations. A normal fault system in the eastern part of the line distributes offset (∼150 m) towards the surface along smaller amplitude (tens of metres) antithetic and synthetic faults. In the upper part of the section, a very strong reflector is observed reaching the syncline centre at ∼700 m depth. Its westward surface prolongation corresponds to the contact between the Lower Pleistocene gravels of the Candesti formation (e.g. Necea *et al*, 2005) and fine-grained sands and silts of Romanian age (Figs 2–4). The contact is conformable in the seismic line, even though further north (north of Suşiţa valley, Fig. 2) this formation unconformably covers the older strata. In contrast, a clear intra-Quaternary unconformity can be observed at the base of the Middle-Upper Pleistocene loess (Fig. 5).

The Rîmnicu Sărat section basically images a large, E-ward-dipping monoclinal structure, with inclinations of beds gradually decreasing towards the E (Fig. 6b). Horizons are continuous and sub-parallel with basically no sign of onlaps to indicate tectonic tilting during deposition of the strata. In the upper, easternmost part of the section a velocity contrast between the Middle-Upper Pleistocene loess and the Lower Pleistocene gravels is clearly marked by a high-amplitude reflector associated with the gravels. The sheet-flow-type gravel-sandstone alternation induces

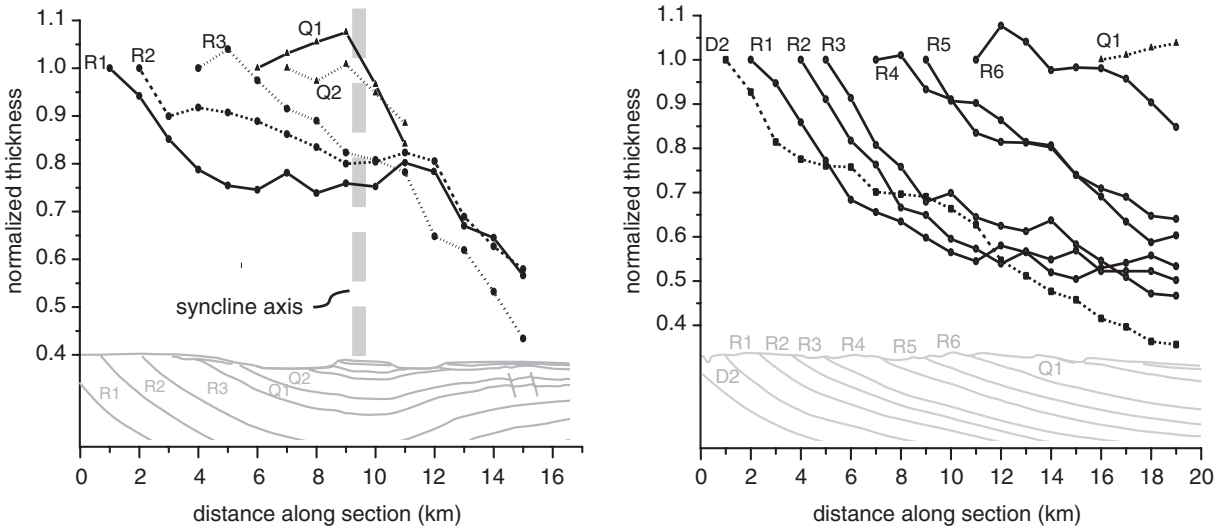

Fig. 9. Normalized orthogonal thickness along depth-converted seismic sections. (a)Putna section. R1-3, intra-Romanian; Q1-2, Quaternary. Note eastward-decreasing thickness for intra-Romanian strata in contrast with Quaternary layers that are thickest around the syncline axis. (b) Rîmnicu Sărat section. D2, Dacian; R1-6, intra-Romanian; Q1, Quaternary. Eastward-thinning trend is again restricted to Pliocene sediments.

remarkably high-amplitude reflectors due to internal contrasts in lithology. Middle-Upper Pleistocene deposits display onlap/offlap patterns, where the E-ward thickening is locally associated with proximal onlaps, indicating a syntectonic/folding character.

We analysed the lateral thickness changes by measuring the orthogonal thickness of the interpreted intervals along the depth-converted sections. Along the Putna section (Fig. 9a), measurements were stopped west of the faulted zone. For better comparison, the measured thicknesses were normalized with respect to their westernmost value. In both sections, the Pliocene intervals show an eastwards-thinning trend, with up to a 60% decrease (horizon D2 in section D, Fig. 9b). Along the Putna section, the eastward thinning along the Romanian intervals is irregular, the fastest thinning taking place in the eastern part of the section (from 11 km). The Quaternary intervals show a different pattern in that they are thickest around the syncline axis (9 km). This indicates an early Quaternary eastward shift of the basin depocentre. Thickness changes in the Rîmnicu Sărat section are more regular. The thickness changes are largest in the western part of the section for the oldest intervals (D2, R1-3). This pattern starts to change for the younger Romanian intervals (R4-6), and the thickness Quaternary interval even increases towards the east, again indicating an early Quaternary (Late Pliocene?) shift of the depocentre.

Transition between the Focşani Basin and the East Carpathians orogen

The overall picture derived from the two high-resolution seismic sections is confirmed by industry lines such as the one situated immediately westwards of the Quaternary depocentre of the Focşani Basin (Fig. 10). This line images the westernmost part of the Focşani Basin, characterized by a series of parallel reflectors, from the steeply dipping, continuous and high-amplitude Upper Sarmatian reflectors to more gently dipping, lower-amplitude Romanian strata. In the W, the steepened lower portion of the Focşani Depression is in contact with a complex of thrust sheets belonging to the Subcarpathian nappe, bounded at its base by the Pericarpathian thrust.

In the upper part of the interpreted section (Fig. 10b and c), west-dipping Subcarpathian nappes tectonically overlie the E-ward steepened sediments of the Focşani Depression. In the field, this contact (at ~7 km from the western termination of the line) is poorly exposed all along the

Fig. 10. Interpreted deep seismic line B at the contact between the thin-skinned thrust belt and the western flank of the Focşani basin (location in Figs 2 and 3). Seismic and velocity data courtesy of Forest Oil International and Romanian National Agency for Mineral Resources. (a) Seismic line, vertical scale in seconds TWT; (b) line drawing and interpretation. (c) Depth-converted interpretation. Conversion in depth was made using average interval velocities derived from neighbouring wells (e.g. Tărăpoancă *et al*., 2003). Vertical scale in kilomrtres, no exaggeration. Pg, Palaeogene; Ec, Eocene; Ol, Oligocene; Bd, Burdigalian; Bn, Badenian; Sm_1, Lower Sarmatian. Sediments corresponding to the actual foredeep succession (Lower-Middle Sarmatian) are shaded grey. Interpretation of outcropping part of Subcarpathian Nappe further constrained by surface observations. No discontinuity is evident between the Sarmatian wedge-top sediments and the overlying parallel-stratified succession. Note the elevated basement position below the thin-skinned belt with respect to the adjacent foreland, attributed to late-stage Quaternary out-of-sequence basement-involved faulting and folding of the entire system. Further description in the text.

western flank of the FD. In the Putna valley, the contact is marked by a breccia of clastic rocks dragged by diapirs of Lower Miocene salt rising along the contact during and after nappe emplacement ('salt-breccia', e.g. Mrazec, 1907; Ştefănescu *et al*., 2000). Rocks are highly deformed and do not provide consistent kinematic indicators. Across the contact, over a distance of ~500 m towards the W, the outcropping strata change from subvertical, well-exposed

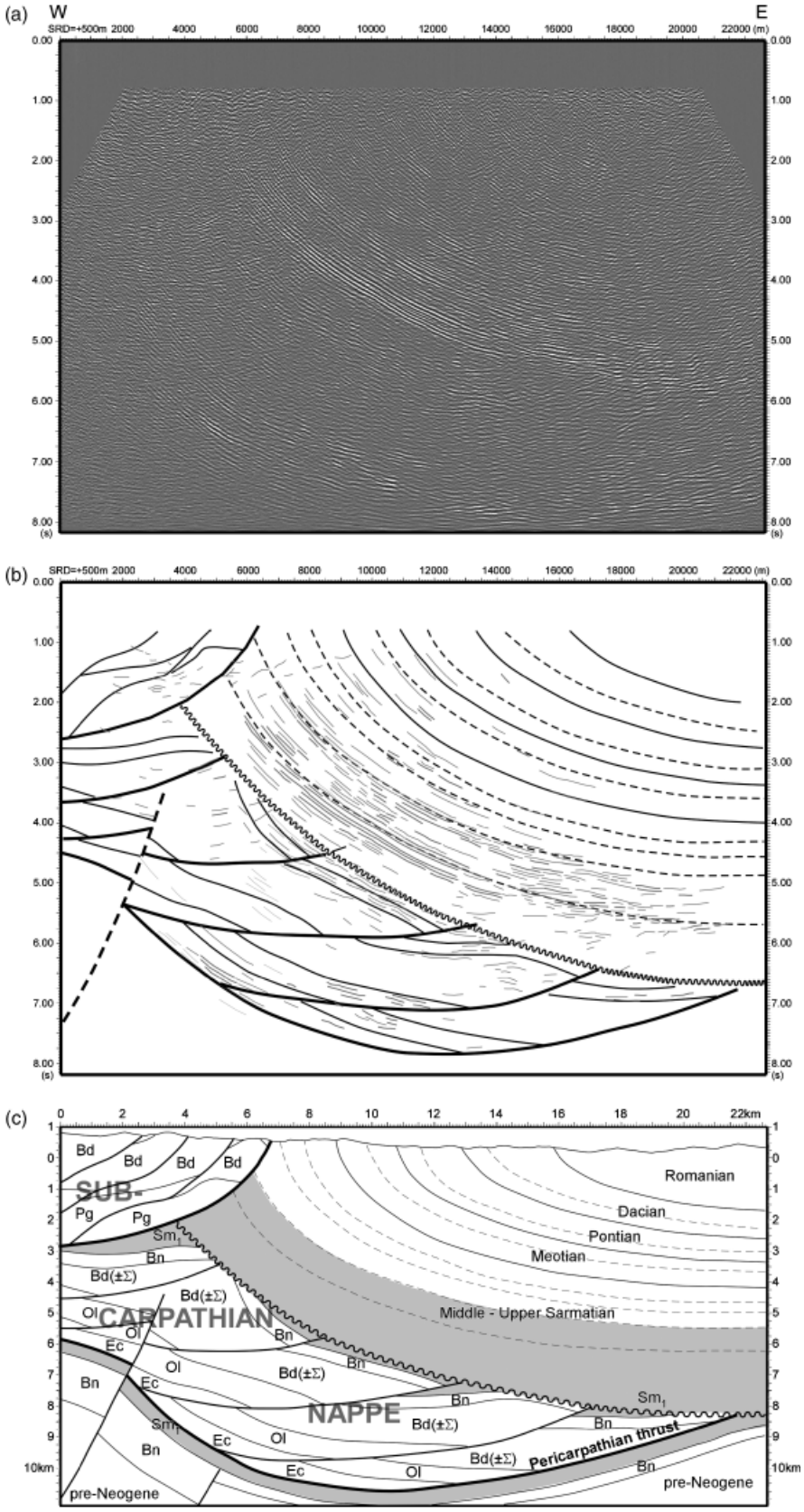

calcareous Upper Sarmatian sandstones to highly deformed and roughly westward-dipping, Lower Miocene fine-grained sandstones and clays. Internal deformation of the latter consistently indicates an eastward direction of thrusting (e.g. Morley, 1996). Determining the internal geometry of the thrust sheets is not straightforward from this seismic line. Four thrust sheets with 100–200 m offsets are inferred in the hanging-wall of the frontal-exposed thrust by surface correlation.

In the lower part of the section, the substratum of the outcropping Subcarpathian nappes and of the Focşani sequence shows reflectors of generally low amplitude, steepening from E to W, similar to the trend of the overlying sediments. The interpretation of this part of the section is based on correlation of the seismic facies to the deposits in other frontal zones of the Subcarpathian nappe where the seismic lines are controlled by wells (such as the Buzau-Teleajen area, see Ştefănescu *et al.*, 2000). High-amplitude, low-frequency reflectors, corresponding to Oligocene sandstone-shale alternance, are truncated by thrust faults in the centre of the section at depths of 6–8 s (Fig. 10a). The overlying seismically transparent level corresponds to Burdigalian salt and low-contrast turbidites, covered in turn by more reflective Upper Badenian sandstones.

The nature of the contact between the thrust complex and the sediments of the Focşani Depression, in the deepest part of the basin overlying the frontal part of the wedge, is difficult to determine unambiguously from this line. Truncations of reflectors are observed below a transparent interval around 10 km (5 s)$^{-1}$ TWT, suggesting an erosional unconformity. A similar intra-Sarmatian unconformity was interpreted by Ştefănescu *et al.* (2000) in the southern part of the Bend Zone. A favourable alternative interpretation, again derived from observations in the southern part of the Bend Zone (Profiles X and XI in Matenco & Bertotti, 2000), is that of a wedge top depozone sensu DeCelles & Giles (1996): Sarmatian sediments were deposited on top of the frontal part of the actively deforming Subcarpathian Nappe. In any case, the backthrust that was previously proposed by Matenco & Bertotti (2000) can be excluded from these seismic data: at the surface, the tilted Focsani succession is overridden by an east-vergent thrust.

Below the Pericarpathian thrust at the base of the deformed wedge, our interpretation is speculative. However, the fault-controlled increase in thickness in Badenian sediments was imaged by deep seismic studies (Bocin *et al.*, 2005) and inferred by Tărăpoancă *et al.* (2003). The most remarkable feature is the position of the Pericarpathian thrust itself, at $\sim$6 km depth in the western part of the section and deepening to $>$ 10 km towards the east, constrained by the interpretation of deep crustal reflection lines, which indicate in this area a velocity increase from 2–3 to 5 km s^{-1} (Bocin *et al.*, 2005; Panea *et al.*, 2005), characteristic for the limit between the Neogene evapourites/clastics and the Mesozoic carbonates. Although it is not well controlled by the seismic line, based on the studies cited above a basement-involved reverse fault has additionally been interpreted. The basement and the Pericarpathian thrust are displaced by this steep, W-dipping reverse fault which accommodates a displacement of $<$ 500 m.

Recent active faulting along the eastern flank of the Focşani Basin

The Independenţa line (line A, Fig. 7, location in Fig. 2) shows the eastern termination of the Focşani Basin, imaged by the progressive eastward thinning of all sedimentary units. Thinning is partly accommodated by a large number of normal faults with offsets (in the section plane) in the order of tens of metres at the base Quaternary level, sometimes increasing at depth. These faults belong to the system of the Peceneaga-Camena fault (Fig. 2, Matenco *et al.*, in press). The most remarkable feature is the fault in the central-eastern part of the line (at 10 km), associated with large roll-over antithetic tilting of Quaternary strata, which caused a difference in surface topographic elevation similar to its offset ($\sim$100 m). At depth, the offset at the base Neogene unconformity level is higher ($\sim$300 m), indicating that Quaternary faulting reactivates a previous Sarmatian event. Most of the other normal faults truncating the upper sequences only caused thickness changes in the Quaternary series, which points to a Quaternary activation. Earlier normal faults, presently inactive, can be observed at the Sarmatian, and subordinately at the Badenian level. These faults were probably created during the Badenian extension (Tărăpoancă *et al.*, 2003) and subsequent Sarmatian normal faulting related to thrust loading (Leever *et al.*, 2006), locally involving a limited amount of dextral strike–slip movement (see also Tărăpoancă *et al.*, 2003). The latter might explain the structural inversion (lower syncline, upper anticline) observed in the Sarmatian in the central-western part of the section (at 4–5 km).

Overall, the Quaternary (to present day) deformations are distributed along numerous normal faults in a wide zone of deformation with clear topographic expression.

REGIONAL CROSS SECTIONS AND RESTORATIONS

The shallow seismic data provide a new and very detailed picture of the architecture of the western flank of the Focşani Depression adjacent to the Carpathians fold-and-thrust belt. In the following, we integrate the new seismic data with literature sources to construct a couple of sections from the western part of the Focşani Depression to the internal nappes of the East Carpathians. Restoration of these sections images the kinematic late orogenic evolution of the Carpathian Bend Zone. We distinguish between the Lower-Middle Sarmatian sediments that were deposited in the actual foredeep, where the generation of accommodation space was directly related to deflection of the lower plate as a result of orogenic loading, and the younger,

late-orogenic Focsani succession, for which the accommodation space is not genetically linked to the Carpathian collision.

Geological cross sections from E-Transylvania into the Focşani Basin

In order to derive an overall picture of the late orogenic deformations that affected the belt and its foreland as a single unit, two regional cross-sections (Fig. 11) were constructed. They start in the west in the Quaternary Tirgu Secuiesc Basin, that unconformably overlies the internal nappes of the East Carpathians. They then traverse the outer Moldavidian nappes and continue into the Focşani Basin (Fig. 2). The cross-sections incorporate the two high-resolution seismic lines along the western Focşani flank.

Data used for construction of the cross-sections were taken both from the seismic interpretations presented above and from literature sources. The structure of the frontal (Tarcău, Marginal Folds and Subcarpathian) nappes was extrapolated at depth from surface information available from existing geological maps. This extrapolation was correlated with interpretations of Dicea (1995), Matenco & Bertotti (2000) for the detailed architecture of the thrust sheets, and with those from Rădulescu *et al.* (1976), Bocin *et al.* (2005), Panea *et al.* (2005) and Hauser *et al.* (2001) for the position and structural geometry of the basement of the lower plate, beneath the thrust sheets. The overall structure of the Focşani Basin east of our lines was taken from Tărăpoancă *et al.* (2003) and Matenco *et al.* (2003, 2005).

From W to E, the sections show the Tarcau, Marginal Folds and Subcarpathian nappes, which are part of the Moldavidian tectonic units (Săndulescu, 1988) deformed in the Neogene. They are overridden by more internal units in the extreme western part of the sections. In the east, the tilted autochtonous foredeep succession partly overlies the frontal part of the wedge. Significant (>40 km) late Miocene underthrusting is evident from the far westward extent of the Badenian sediments in the basement.

In the northern section (Fig. 11a), the Marginal Folds nappe crops out in the Vrancea Window (Fig. 3). Along the southern section (Fig. 11b) and further south, this nappe no longer crops out; it laterally wedged out. Here, the internal deformation in the Tarcau nappe is mainly accommodated by backthrusts (Fig. 11b).

Both sections show the folded middle Sarmatian–Quaternary foredeep sediments overlying the frontal part of the flysch belt, the Subcarpathian nappe. The Lower Sarmatian sediments (sm_1) are coarse-grained calcareous sandstones from a deltaic environment and represent the actual foredeep succession, occurring both as deformed wedge top sediments (Ford, 2004; DeCelles & Giles, 1996, Fig. 11b) and adjacent to the wedge in the foredeep depozone, reaching thicknesses of 2–3 km. As noted in section *Transition between the Focşani Basin and the East Carpathians orogen*, the resolution of the seismic line that images the contact between the frontal part of the wedge and the Focsani succession, is not sufficient to determine unambiguously the nature of the contact. The alternative interpretations: an erosional contact or wedge top deposition, does not have significant implications for the kinematics. The interpretation of an erosional unconformity between the wedge top and the Middle Sarmatian sediments implies that collision resulted in uplift and exhumation of the frontal part of the wedge (Figs 12f and 13f). Middle Sarmatian out-of-sequence thrusting was accompanied by subsidence of the frontal part of the wedge (Figs 12e and 13e). The interpretation of wedge top deposition would imply continuous subsidence of the frontal part of the wedge since Sarmatian collision.

The basement of the flysch belt and its foredeep, the Moesian Platform, has an undulating shape, occurring at a shallow depth (6–7 km) below the thrust belt in the west and at more than 11 km at the frontal part of the wedge. It is dissected by normal faults that have been reactivated as reverse faults in the western part of the sections, displacing the Badenian–lower Sarmatian detachment level below the allochtonous flysch belt by 1–2 km upwards (e.g. at 30 and 50 km in Fig. 11a). Movement along these faults partly accommodates the basement uplift below the wedge. The northern section (Fig. 11a) shows the eastern limit of the basin at the Peceneaga-Camena fault system.

Restoration of the cross sections: method and constraints

Palinspastic restoration of the two lines (Figs 12 and 13) was performed using 2D Move, assuming flexural slip unfolding (e.g. Suppe, 1983) combined with a fault parallel flow mechanism (Egan *et al.*, 1997) to restore the thrusting movements. The Latest Miocene–Late Pliocene subsidence was restored using a simple vertical shear mechanism. Decompaction and palaeobathymetry were generally ignored, but errors induced are probably relatively minor, as the entire late orogenic succession is characterized by shallow water sediments (cf. Allen & Allen, 2002, Chapter 8).

Restoration of Quaternary-age folding was achieved by (a) removing the Quaternary sediments from the Focşani Depression, (b) tilting the upper Pliocene beds back to horizontal including the underlying thrust system and basement and (c) compensating for exhumation/uplift in the western part of the section, including restoration of the deep reverse faults. A displacement of $\sim$1.5 km along the frontal-exposed Subcarpathian thrust was suggested and required by the restoration. The restoration implies a total amount of thick-skinned Quaternary shortening of 4–5 km, in agreement with the values inferred by e.g. Matenco & Bertotti (2000) for the Wallachian phase. The Quaternary basement uplift in the western part of the section is constrained by low-temperature thermochronology, which provides an estimate of *ca.* 5 km of exhumation experienced by the presently exposed nappe system during

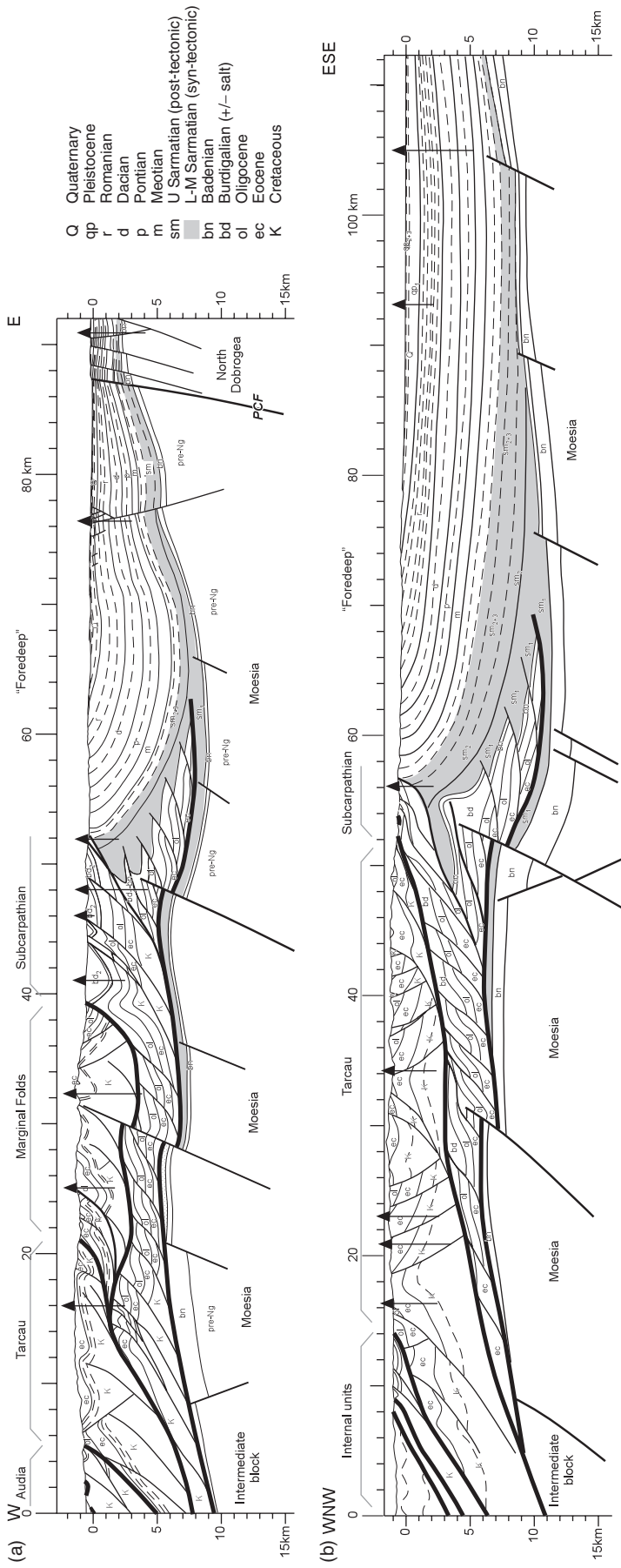

Fig. 11. Regional geological cross sections of the external thrust nappes and the adjacent Focşani foreland (locations in Fig. 2). Depth information is derived from the shallow seismic results of the present study and Dicea (1995), Matenco & Bertotti (2000), Tărăpoancă *et al.* (2003), Tărăpoancă (2004), Bocin *et al.* (2005) and Panea *et al.* (2005). Projected wells are shown. Intermediate block senso Visarion *et al.* (1988). (a) Regional cross section enclosing the Putna shallow seismic line (Fig. 5). (b) Regional cross section enclosing the Râmnicu Sărat shallow seismic line (Fig. 6). Sediments corresponding to collision stage shaded grey. Description in the text.

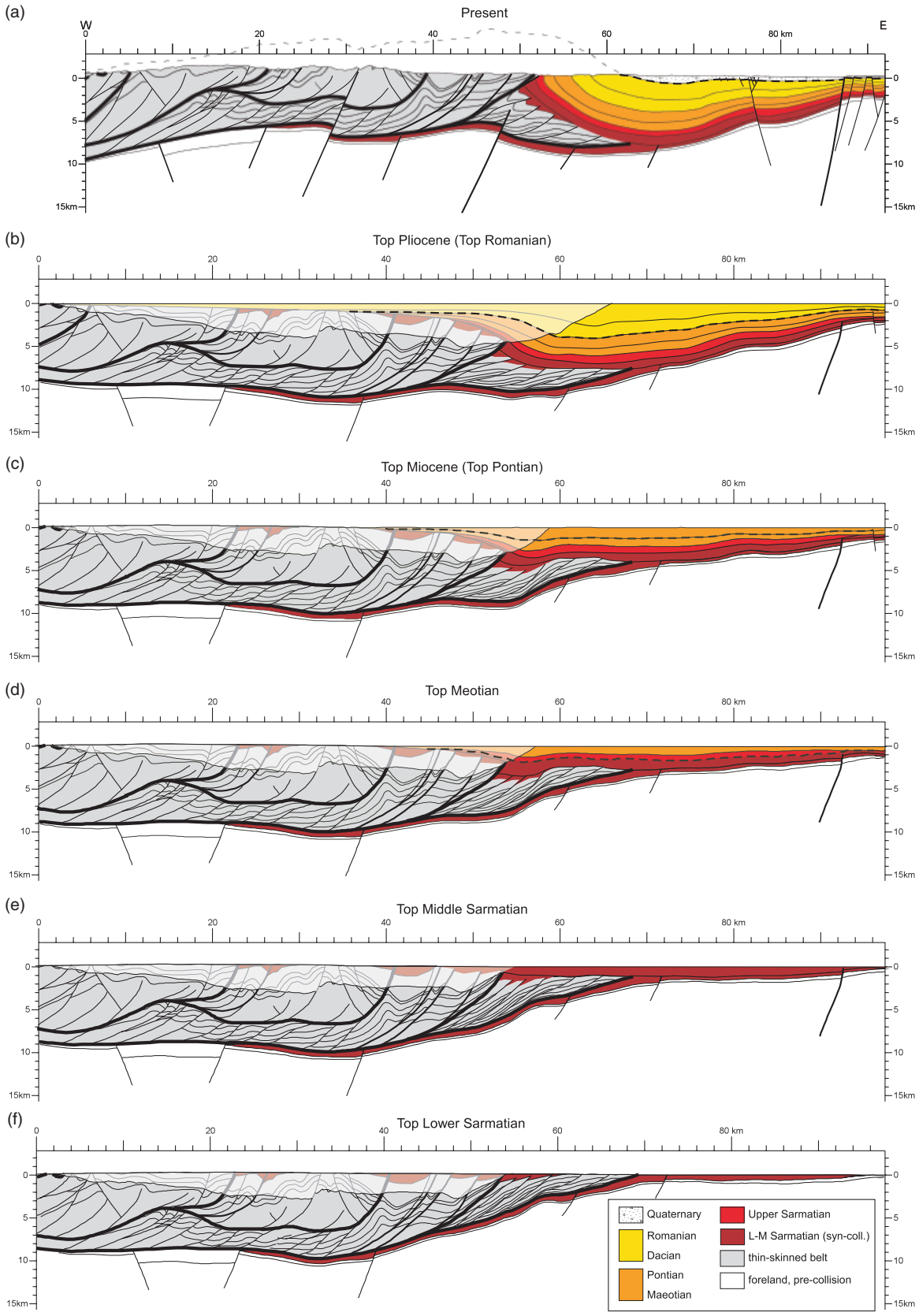

Fig. 12. Restoration of the post-nappe stacking evolution of the northern cross section (along the Putna section, Figs 5 and 11a). The restoration shows the two different stages of late orogenic evolution: Latest Miocene–Pliocene general subsidence (d–b) followed by 5 km of Quaternary shortening and tilting (a). Further description in the text.

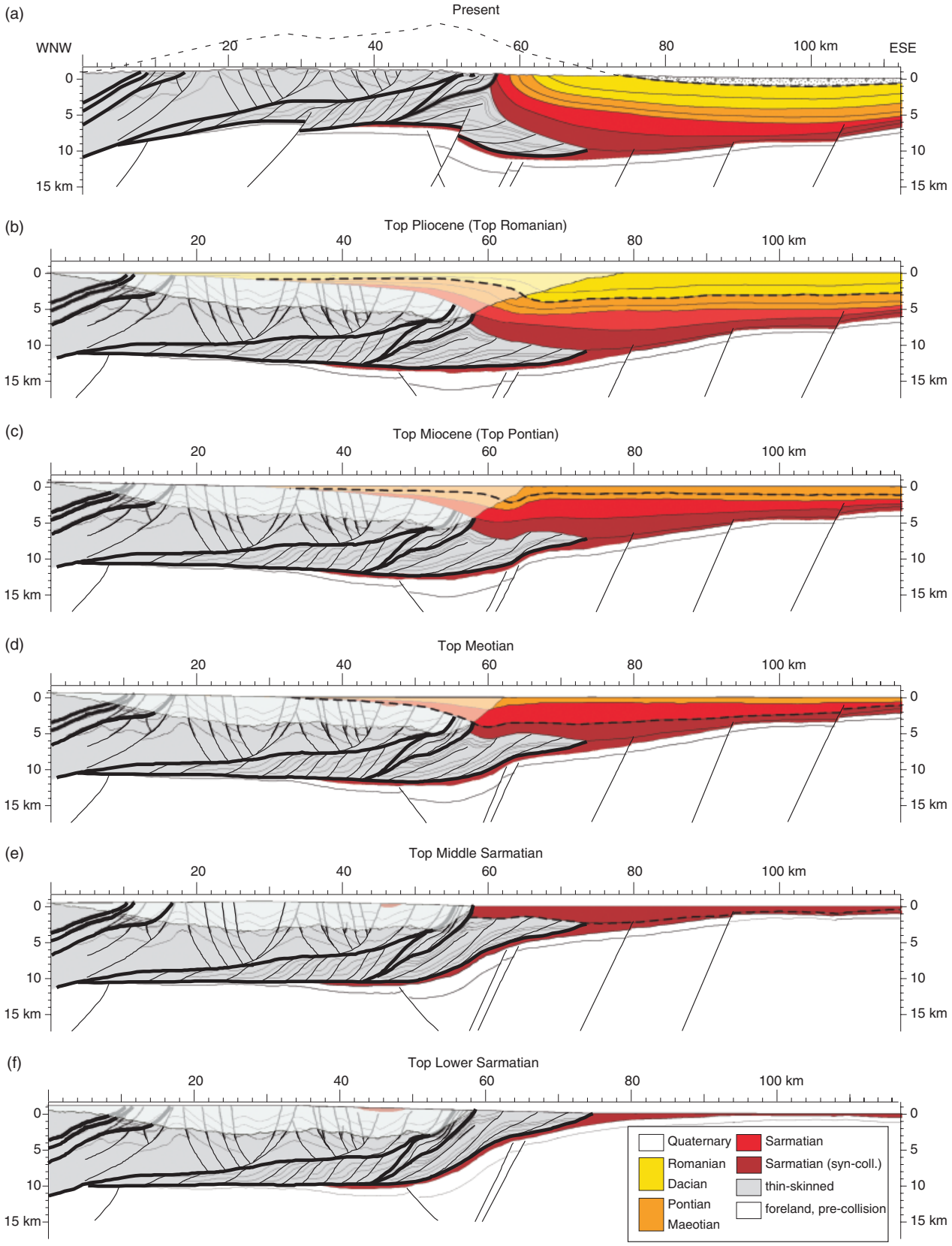

Fig. 13. Restoration of the post-nappe stacking evolution of the southern cross section (along the Râmnicu Sărat section, Figs 6 and 11b). The restoration shows the two different stages of postorogenic evolution: Latest Miocene–Pliocene general subsidence (d–b), followed by 5 km of Quaternary shortening and tilting (a). Further description in the text.

Quaternary times (U–Th/He and apatite fission track data from Sanders *et al.*, 1999; Merten *et al.*, 2005). The space obtained between the present day and top-Pliocene surface positions was speculatively filled with the eroded part of the nappe system and with sediments of the Focşani Depression.

The reconstruction of the Romanian-age (Figs 12b and 13b) geometry of the eroded part of the Focşani Basin, extending west over the entire length of the section, is constrained by the fauna of the pre-Quaternary sediments of the Brasov and Tirgu Secuiesc Basins (location in Figs 1 and 2). The Pliocene lacustrine sediments in these basins contain fauna assemblages similar to the ones in the Dacic Basin (i.e. Focşani type; Marinescu & Papaianopol, 1995; Olteanu, 2003), requiring a connection between the basins across the present-day orogen.

The subsequent stages (Figs 12 and 13c–f) were reconstructed by flexural slip unfolding after stepwise removal of the sediment overburden.

Kinematic evolution: patterns of vertical movements and horizontal deformations

During the last stages of nappe emplacement, the thin-skinned wedge had reached the stable Moesian platform (Figs 12 and 13e–f). The wedge has a thickness of 2–3 km in its frontal part (see also Dicea, 1995; Matenco & Bertotti, 2000) and is gradually thickening westwards, its elevation close to sea level. The syntectonic Lower Sarmatian sediments occur below and in front of the wedge front, and on top of it in intramontaneous (piggy back) basins. Erosion affects the exposed parts of the actively deforming wedge. Subsidence was accompanied by local normal faulting, such as along the Peceneaga–Camena fault in the Putna profile (Fig. 12e).

The Upper Sarmatian–Pliocene period (Figs 12 and 13d–b) was characterized by homogeneous subsidence. Sediments were deposited in a generally lacustrine environment. In our reconstruction, the resulting large and deep sedimentary basin extends well over the present-day orogen. In the Late Pliocene, the western margin of the proto-Focşani Depression lies only a few kilometres from the Transylvania Basin, leaving little space for a pronounced morphology in the SE Carpathians.

The pattern of vertical movements changed significantly at the beginning of the Quaternary when subsidence in the western part of the proto-Focşani Depression changed to uplift (compare Figs 12 and 13b and a). The present-day undulated geometry of the main sole thrust and its deepest point in an apparently unrealistic external position (see Bocin *et al.*, 2005) do not reflect the situation during nappe emplacement. Rather, it is due to the Quaternary differential uplift and subsidence associated with a total shortening of some 5 km. An anticline–syncline couple was formed by uplift in the thrust belt and subsidence in the foredeep.

Uplift of the orogen was partly accommodated by reverse faulting in the core of the anticline. The faults have an offset of $\sim$2 km. Displacement along these faults is transferred to the surface by folding in mechanically weak layers. Tilting of the western flank of the present-day Focşani Depression resulted from this uplift, whereas subsidence continued in the core of the syncline that evolved to the east of the uplifting zone. The syncline core defines the position of the Quaternary depocentre. In the western flank of the syncline, the inclination of pre-Quaternary sediments ranges from 15 to 20° in Romanian layers to subvertical in Upper Sarmatian. Our reconstruction attributes $\sim$65° of the tilting of the Sarmatian strata to the Quaternary events (Figs 12a and 13a), which implies that $\sim$25° tilting must have been previously acquired by differential subsidence in Latest Miocene-Pliocene times (Figs 12 and 13b and c). Total uplift of the orogen accumulates to $\sim$5 km, the maximum subsidence in the basin amounts to 2 km. The Quaternary folding is asymmetric, with gentle western and steep eastern flanks. An alternative mechanism that was proposed previously, invokes low-angle thrusts to explain the exhumation of the Vrancea half window (Fig. 2, Roure *et al.*, 1993) and could also explain the elevated basement position below the belt. However, due to the lower angle faults, this mechanism requires a much larger amount (20 km) of shortening to explain the observed Quaternary uplift.

DISCUSSION

The restoration of geometries and timing of vertical movements in the transition zone between the Carpathian Bend and the adjacent Focşani Depression has shown that most of the subsidence in the foreland and subsequent exhumation/uplift in the mountains took place after cessation of major shortening in the Middle Sarmatian (Figs 12 and 13). We were able to distinguish a first Latest Miocene–Pliocene stage characterized by generalized subsidence of the entire area adjacent to and including the present-day thrust belt, and a second, Quaternary, stage characterized by exhumation and uplift in the internal sectors and ongoing subsidence in the centre of the present-day Focşani Basin. In the following, we present our results in the regional geodynamic framework.

Regional Latest Miocene–Pliocene subsidence in the Moesian domain

The first period of Latest Miocene-Pliocene (Late Sarmatian–Romanian) subsidence is common to the entire Moesian domain but shows exaggerated values in the Focşani Basin (Figs 12 and 13e–b). Adjacent to the South Carpathians, the Getic Depression is characterized by extensive Sarmatian wedge-top sedimentation and up to 1 km of late orogenic sediments (Răbăgia & Matenco, 1999). The foredeep of the East Carpathians, from the end of contraction, was gradually filled towards the south. Upper Sarmatian sediments showing southward prograding deltaic structures occur as far north as Piatra Neamt (47°N, Tără-

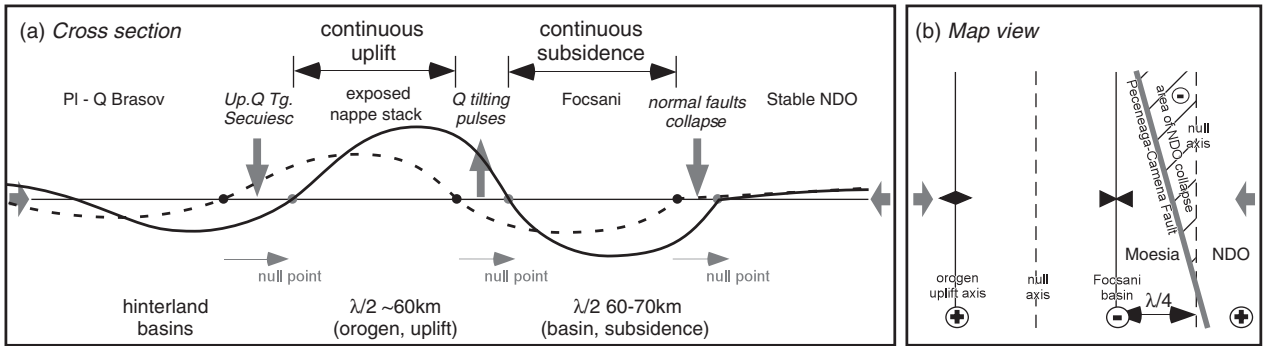

Fig. 14. Schematic representation of the migrating Quaternary folding in the external East Carpathians and their foreland. NDO, North Dobrogea Orogen. (a) Upper Quaternary migration of the folding null point; (b) map view: Wavelength re-equilibration on the eastern flank of the Focşani basin through the collapse by normal faulting of the NNE part of the North Dobrogea Orogen, near the oblique Peceneaga–Camena fault. The area of faulting is the widest in the north, where a larger part of the NDO basement block has been affected by the eastward-migrating folding-related subsidence or null axis.

poancă, 2004), whereas Meotian–Dacian sedimentation is constrained to the Moesian platform, south of the Trotus fault (Fig. 2). In the Focşani Depression, postcollisional subsidence has thus created a basin with upto6 km of sediments (Tărăpoancă *et al*., 2003) in the almost total absence of any genetically related faults. On the west flank of the Bend Zone, the Brasov Basin accumulated up to 300 m of Pliocene lacustrine sediments, its fauna showing a connection with the Focşani Basin at that time (Marinescu *et al*., 1981; Figs 12 and 13b). From our sections, we reconstructed the approximate position of the Latest Miocene–Pliocene depocentre (Figs 12, 13d–b and 14).

Quaternary contraction and inversion in the Pannonian–Carpathian system

In the early Quaternary, the patterns of uplift and subsidence changed significantly. Deposition of coarse-grained continental–shallow lacustrine gravels and sands (Candesti formation, see also Marinescu *et al*., 1981; Necea *et al*., 2005) strongly contrasts with the Late Pliocene depositional environment of fine-grained lake sediments. This coarse facies points to a new proximal source area, i.e. the emerging hinterland. In our seismic sections, the gravels conformably overlie the lower series, but further to the north and west the contact is unconformable. The gravels crop out at present elevations of up to 1000 m, where they dip towards the east at $\sim 9^{\circ}$.

Uplift and erosion started west of the present-day basin margin and supplied the coarse-grained sediments. In time, it migrated eastward, also affecting the newly deposited Candesti gravels, uplifting and tilting it to its present elevation and angle. The axis of the resulting syncline (Fig. 5) is the depocentre for the Candesti conglomerates and represents an area of continuous Pliocene–Lower Quaternary subsidence. Currently, the syncline axis resides in the foothills and is incised by the Putna and Susita rivers (Fig. 14a). Middle-Upper Pleistocene loess deposits unconformably overlie (in Putna section at 12 km, Fig. 5) the lower Quaternary deposits, indicating a subaerial (uplifted) position of the former depocentre at that time. Recent detailed geomorphological studies distinguished three stages for the Quaternary tilting (Necea *et al*., 2005).

The present-day area of maximum subsidence, monitored by GPS measurements (subsidence rate up to 3 mm year^{-1}, Van der Hoeven *et al*., 2005), is located even further to the east and corresponds to the area of minimum topography along the Siret river at 2.5 m above sea level. Its tributaries (Rîmnicu Sărat, Buzau) are reorienting towards this zone (Fig. 14a, Fielitz & Seghedi, 2005), whereas Siret itself has migrated eastwards, as shown by the abandoned Upper Pleistocene–Holocene river meanders (Matenco *et al*., in press) and the steep escarpments on its eastern flank.

The Quaternary–recent foredeep subsidence is not transferred to the buried prolongation of the North Dobrogea Orogen (NDO), which shows a limited uplift as suggested by GPS measurements (1–2 mm year^{-1}, Van der Hoeven *et al*., 2005). The difference between the relatively stable NDO and subsiding Moesia is accommodated by a large normal fault system (Fig. 2), much wider in the north in the prolongation of the Putna cross section than further south where it is crossed by the Independenţa seismic line (Fig. 7). As shown in this seismic line and in the restored Putna section (Fig. 12), the fault system was initially activated during Sarmatian times, only along the main trace of the Peceneaga-Camena fault. During the Quaternary, a larger area east of this fault has been affected, creating this wide system of normal faults. Across the fault zone from west to east, the age of the outcropping sediments increases from lower Holocene–Upper Pleistocene–Middle Pleistocene (Fig. 2).

Mechanisms for the two-stage Latest Miocene-recent evolution of the Focsani area

A large number of qualitative models have been proposed to explain the unusual features in the SE Carpathians. These models involve mechanisms such as roll-back of an oceanic lower plate [e.g., Royden, 1993 (continental)

delamination Girbacea & Frisch, 1998; Chalot-Prat & Girbacea, 2000; Gvirtzman, 2002; Knapp *et al*., 2005, slab tear and detachment Wortel & Spakman, 2000], or a thermally re-equilibrating slab (Cloetingh *et al*., 2004). We will briefly discuss the implications of our new constraints on the magnitude and timing of vertical movements and tilting in the area on the existing models that did not recognize the two separate stages, and propose an alternative explanation.

The model of Royden (1993) associates deep foreland basins with roll-back of the subducting plate. However, as roll-back is active during underthrusting and necessarily stops after collision, this mechanism could not explain the large amount of post-orogenic sediments in the Focşani Depression. A similar problem in timing arises for the delamination models. These imply (Girbacea & Frisch, 1998; Chalot-Prat & Girbacea, 2000) that extension in the Brasov/Tirgu Sequiesc Basins due to magmatic doming is simultaneous with subsidence in the Focşani Basin and tilting of its western flank. The events are placed in Sarmatian time. Slab break-off, finally (Wortel & Spakman, 2000), would result in generalized uplift and not the uplift-subsidence couple we observe. For further discussion of lithospheric mantle control on vertical movements, see Bertotti *et al*. (2003). We do agree that the downward force exerted by the remnant, steepened slab as recognized on tomography (e.g. Weidle *et al*., 2005) is the cause for the anomalous Latest Sarmatian–Pliocene and ongoing subsidence.

However, the shallow position of the basement below the wedge (Bocin *et al*., 2005) and the changed patterns of vertical motions in the second evolutionary stage (see section *Kinematic evolution: patterns of vertical movements and horizontal deformations*) are not easily associated with slab control. They do correlate with the contractional episode widely known at the entire Carpathian–Pannonian scale as the second inversion moment (e.g. Horváth, 1993). The age of this event in our study area is Quaternary, whereas elsewhere it started locally during the Pliocene. The magnitude of the Quaternary differential vertical motions in the Carpathian Bend Zone is up to 7 km. Up to 2-km subsidence in the foredeep is constrained by our seismic data, and 5 km of erosion in the adjacent orogen is constrained by thermochronology (Sanders *et al*., 1999) and corroborated by our reconstructions. Similar coeval patterns of subsidence and uplift as in the Carpathian Bend Zone, but of reduced magnitude, are known in the <500-m thick, Pliocene-Quaternary Tisza sub-basin of the Great Hungarian plain (e.g. Horváth & Cloetingh, 1996; Thamó-Bozsó *et al*., 2002), and the actively uplifting Transdanubian Central Range (e.g. Fodor *et al*., 2005; Ruszkiczay-Rüdiger *et al*., 2005).

The mechanism responsible for the Quaternary differential vertical movements in the Pannonian domain has been previously inferred as crustal/lithospheric buckling (e.g., Horváth & Cloetingh, 1996; Bertotti *et al*., 2003; Cloetingh *et al*., 2004). The compressional stress field responsible is most commonly explained by the Adriatic plate push and redistribution of the stress field in a weak Carpathians–Pannonian domain (e.g., Bada *et al*., 1999). Our observations in the Bend Zone support this folding mechanism as a reasonable explanation of the eastward-migrating patterns of uplift and subsidence.

Although the recent uplift of the Bend Zone, with its highest relief centered on the earthquake hypocentres might be explained by one of the (detaching) slab models (see e.g. Bertotti *et al*., 2003), the geometry of the steeply tilted western flank of the Focşani depression and in particular the syncline in the northern section (Fig. 5) can only be explained by compressional folding. Moreover, from the positions of the Latest Miocene–Recent depocentres, an eastward migration of the uplift-subsidence couple is evident. The wavelength of the Quaternary folding can be estimated from the width of the subsiding and uplifting regions (Fig. 14). The migration of the folding is expressed in the following as the migration of its 'null points', which separate regions of uplift and subsidence, and where, as a consequence vertical movements are zero.

Folding: wavelength and time migration

From our reconstructions for the Pliocene–Pleistocene transition (Figs 12 and 13a and b), the position of the null point to the east of the anticline uplifting the orogen and tilting the western Focşani flank is difficult to estimate, but it must have been to the west of the presently exposed Candesti gravels. It migrated eastwards during the Quaternary, folding the lower Pleistocene strata and finally causing a gradual tilting of Pleistocene–Holocene strata (Necea *et al*., 2005). On the west side of the orogen, the <500-m thick Pliocene–Quaternary Brasov Basin is connected on its eastern margin with the <100-m thick Upper Quaternary Tîrgu Secuiesc Basin (Fig. 14a). The present surface elevation of the Brasov Basin is at 500 m, having accumulated up to 200 m of continental Quaternary sediments (Ghenea *et al*., 1979, Chalot-Prat & Girbacea, 2000) and experienced a net uplift of 300 m since the end of the Pliocene. The E–W extent of Tîrgu Secuiesc Basin gives an indication of the distance that the folding null point has migrated during the Quaternary, $\sim$20 km (Fig. 14a and b).

The geometry of the Quaternary subsidence in the Focşani Basin was directly imaged by our study and starts from the eastward-migrating null point on the western Focşani Basin flank and ends in the east at the Peceneaga–Camena fault. Because this fault is oblique with respect to both the direction of the orogen and the syncline axis, the distance between the null points apparently increases southwards, from $\sim$35 to $\sim$70 km (Figs 12–14a). The key issue here is the previously described Quaternary normal faults system, which accommodates the subsidence of Moesia with respect to the North Dobrogea Orogen. As pointed out by Matenco *et al*. (in press), this system has Quaternary deformation ages younger towards the east. This can be explained in two ways. One explanation is the tendency of the folding mechanisms to widen the subsiding area in

the northern foreland to a similar ~70 km half wavelength as in the south, and comparable with the 60-km value of the inner Carpathians uplift zone. The second potential explanation relates to the striking coincidence of the width of the normal fault system, ~20 km, with the earlier described distance on which the null-point migrates during the Quaternary and with the width of the Targu Secuiesc Basin. In this line of reasoning, the gradual formation of Quaternary normal fault younger in age to the east can be explained as a migration of a third null point eastwards, the one that separates the subsidence in Moesia with the uplift of the North Dobrogea orogen (Fig. 14).

One general conclusion can be drawn whichever are these later mechanisms. The folding has a wavelength of ~120 km and displays a clear eastward migration in time.

CONCLUSIONS

The late orogenic evolution of the external part of the East Carpathians and their foreland is characterized by two distinct periods. A first Latest Miocene–Pliocene (Upper Sarmatian–Romanian) period of generalized subsidence in the entire domain is subsequently followed by < 5 km Quaternary shortening with significant differential vertical movements in the studied area.

The Latest Miocene–Pliocene period of subsidence is common in the entire Moesian domain but shows exaggerated values in the Focşani Basin. This subsidence, most likely driven by the slab below Vrancea, has created a basin with up to 10 km of sediments in the almost total absence of any genetically related faults. The Pliocene Focşani Basin was in connection with the Brasov basin, and the depocentre overlay the frontal part of the thrust belt.

The second, Quaternary, stage of folding is the result of a contractional episode widely known at the entire Carpathian–Pannonian scale as the second inversion moment. The age of this event in our study area is Quaternary, whereas elsewhere it started locally during the Pliocene. It involved differential vertical motions of up to 7 km, comprising up to 2 km subsidence in the foredeep and up to ~5 km of exhumation in the adjacent orogen.

The Quaternary differential vertical movements in the Carpathian–Pannonian domain are attributed to crustal/lithospheric buckling. The compressional stress field responsible is most commonly explained by the Adriatic plate push and redistribution of the stress field in a weak Carpathian–Pannonian domain. In our study area, the response to these overall, regional mechanisms is almost one order of magnitude higher than elsewhere. Two to 5 km of Quaternary uplift of the external part of the SE Carpathians nappe pile and the western flank of the Focşani Basin are coeval with deposition of up to 2 km of sediments in the foreland. The wavelength of the folding mechanism is ~120 km and the points of zero vertical movement of the regional anticline/syncline couple migrated some 20 km eastwards during the Quaternary. The steep eastward dip of the strata on the western Focşani flank of presently vertical positions is partly inherited from earlier differential subsidence, partly acquired during the overall anticlinal growth and partly the result of local structures. Total Quaternary shortening is in the order of 5 km as revealed by our reconstructions and is transferred towards SE and E along dextral strike–slip faults (Matenco *et al*., 2003) and the high-angle reverse faults that are commonly ascribed to the Wallachian deformation (e.g., Hippolyte & Săndulescu, 1996).

ACKNOWLEDGEMENTS

The Netherlands Research Centre for ISES has provided financial support for the acquisition of the high-resolution shallow seismic lines and for supporting the research carried for this publication. SC Prospecţiuni SA that carried out the acquisition and processing, in particular M. Milea and M. Mitroi, are gratefully thanked for the good collaboration and support, and last but not the least for the nice discounts provided in the final price of the lines. The processing team of B. Hărăbor is gratefully acknowledged for professional processing and careful analysis of the acquired data. L. Matenco thanks the very nice and pleasant 'şase, vine clientu' moments spend in the field with the fantastic acquisition team 12 of Prospecţiuni. The knowledge obtained through the collaboration with the University of Bucharest Structural Geology and Basin Analysis team (C. Dinu, V. Mocanu, V. Diaconescu) has often been used in the interpretations. Thanks are also due to Marius Stoica for the palaeontology references. The thorough work and constructive comments of the reviewers, P. Krzywiec, S. Schmid and L. Royden, and the editor, H. Sinclair, were beneficial for the focus and presentation of the manuscript and are greatly appreciated.

This is the Netherlands School of Sedimentary Geology (NSG) publication no. 20061001

REFERENCES

Allen, P.A. & Allen, J.R. (2002) *Basin Analysis: Principles and Applications*. Blackwell Science, London, 451 pp.

Bada, G., Horváth, F., Gerner, P. & Fejes, I. (1999) Review of the present-day geodynamics of the Pannonian Basin; progress and problems. *J. Geodyn.*, **27**, 501–527.

Bala, Z. (1986) Paleotectonic reconstruction of the central Alpine–Mediteranean belt for the Neogene. *Tectonophysics*, **127**, 213–243.

Beaumont, C. (1981) Foreland basins. *Geophys. J. R. Astronom. Soc.*, **65**, 291–329.

Bertotti, G., Matenco, L. & Cloetingh, S. (2003) Vertical movements in and around the SE Carpathian foredeep: lithospheric memory and stress field control. *Terra Nova*, **15**, 299–305.

Bertotti, G., Mosca, P., Juez, J., Polino, R. & Dunai, T. (2006) Oligocene to present kilometres scale subsidence and exhumation of the Ligurian Alps and the Tertiary Piedmont Basin (NW Italy) revealed by apatite (U–Th)/He thermochro-

nology: correlation with regional tectonics. *Terra Nova*, **18**, 18–25.

Bertotti, G., Picotti, V., Chilovi, C., Fantoni, R., Merlini, S. & Mosconi, A. (2001) Neogene to Quaternary sedimentary basins in the south Adriatic (Central Mediterranean): foredeeps and lithospheric buckling. *Tectonics*, **20**, 771–787.

Bocin, A., Stephenson, R., Tryggvason, A., Panea, I., Mocanu, V., Hauser, F. & Matenco, L. (2005) 2.5D seismic velocity modelling in the southeastern Romanian Carpathians Orogen and its foreland. *Tectonophysics*, **410**, 273–291.

Bonini, M. (2001) Passive roof thrusting and forelandward fold propagation in scaled brittle–ductile physical models of thrust wedges. *J. Geophys. Res.*, **106**(B2), 2291–2311.

Burchfiel, B.C. (1976). *Geology of Romania*. Special Paper, 158. Geological Society of America, 82pp.

Cederbom, C.E., Sinclair, H.D., Schlunegger, F. & Rahn, M.K. (2004) Climate-induced rebound and exhumation of the European Alps. *Geology*, **32**(8), 709–712.

Chalot-Prat, F. & Girbacea, R. (2000) Partial delamination of continental mantle lithosphere, uplift-related crust-mantle decoupling, volcanism and basin formation: a new model for the Pliocene-Quaternary evolution of the southern East-Carpathians, Romania. *Tectonophysics*, **327**(1–2), 83–107.

Ciulavu, D., Dinu, C. & Cloetingh, S.A.P.L. (2002) Late Cenozoic tectonic evolution of the Transylvanian basin and northeastern part of the Pannonian basin (Romania): Constraints from seismic profiling and numerical modelling. In: *Neotectonics and surface processes: the Pannonian basin and Alpine/Carpathian system* (Ed. by S.A.P.L. Cloetingh, F. Horváth, G. Bada & A.C. Lankreijer), pp. 105–120. EGU Stephan Mueller Special Publication, Series, 3.

Ciupagea, D., Pauca, M. & Ichmir, T. (1970) *Geologia bazinului Transilvaniei (in Romanian)* Ed. Acad. R.S.R., Bucuresti, 256pp.

Cloetingh, S., Burov, E., Matenco, L., Toussaint, G., Bertotti, G., Andriessen, P.A.M., Wortel, M.J.R. & Spakman, W. (2004) Thermo-mechanical controls on the mode of continental collision in the SE Carpathians (Romania). *Earth Planet. Sci. Lett*, **218**, 57–76.

Csontos, L. (1995) Tertiary tectonic evolution of the Intra-Carpathian area: a review. *Acta Vulcanol.*, **7**, 1–13.

Decelles, P.G. & Giles, K.A. (1996) Foreland basin systems. *Basin Res.*, **8**, 105–123.

Dicea, O. (1995) The structure and hydrocarbon geology of the Romanian East Carpathians border from seismic data. *Petrol. Geosci.*, **1**, 135–143.

Dumitrescu, I. & Săndulescu, M. (1970) *Harta tectonica a României*, 2nd edn. Inst. Geol. si Geofiz., Bucharest.

Egan, S.S., Buddin, T.S., Kane, S.J. & Williams, G.D. (1997) Three-dimensional modelling and visualisation in structural geology: new techniques for restoration and balancing of volumes. Proceedings of the 1996 Geoscience Information Group Conference on Geological Visualisation. *Electron. Geol.*, **1**, 67–82.

Einsele, G. (2000) *Sedimentary Basins: Evolution, Facies and Sediment Budget*, 2nd edn.. Springer Verlag, Berlin, 792pp.

Etris, E.L., Crabtree, N.J. & Dewar, J. (2001) True depth conversion: more than a pretty picture. *CSEG recorder*, **11**, 11–22.

Fielitz, W. & Seghedi, I. (2005) Late Miocene – quaternary volcanism, tectonics and drainage system evolution in the East Carpathians, Romania. *Tectonophysics*, **410**, 111–136.

Flemings, P.B. & Jordan, T.E. (1989) A synthetic stratigraphic model of foreland basin development. *Journal of Geophysical Research*, **94**(B4), 3851–3866.

Fodor, L., Bada, G., Csillag, G., Ruszkiczay-Rüdiger, Z., Horváth, F., Cloetingh, S., Palotás, K., Síkhegyi, F. & Timár, G. (2005) An outline of neotectonic structures and morpho*Tectonics* of the western and central Pannonian basin. *Tectonophysics*, **410**, 15–41.

Fodor, L., Csontos, L., Bada, G., Györfi, I. & Benkovics, L. (1999) Tertiary tectonic evolution of the Pannonian basin system and neighbouring orogens: a new synthesis of paleostress data. In: *The Mediteranean Basins: Tertiary Extension within the Alpine Orogen* (Ed. by B. Durand, L. Jolivet, F. Horvath & M. Seranne), *Geol. Soc. of London Spec. Publ.*, **156**, 295–334.

Ford, M. (2004) Depositional wedge tops: interaction between low basal friction external orogenic wedges and flexural foreland basins. *Basin Research*, **16**, 361–375.

Ghenea, C., Brandabur, T. & Mihaila, N. (1979) *Guidebook for Excursion INQUA*. Geological Institute of Romania, Romania.

Girbacea, R. & Frisch, W. (1998) Slab in the wrong place: lower lithospheric mantle delamination in the last stage of Eastern Carpathians subduction retreat. *Geology*, **26**(7), 611–614.

Gvirtzman, Z. (2002) Partial detachment of a lithospheric root under the southeast Carpathians: toward a better definition of the detachment concept. *Geology*, **30**, 51–54.

Hauser, F., Răileanu, V., Fielitz, W., Bala, A., Prodehl, C., Polonic, G. & Schulze, A. (2001) VRANCEA99 – the crustal structure beneath the southeastern Carpathians and the Moesian Platform from a seismic refraction profile in Romania. *Tectonophysics*, **340**, 233–256.

Hippolyte, J.C. & Săndulescu, M. (1996) Paleostress characterization of the "Wallachian" phase in its type area, southeastern Carpathians, Romania. *Tectonophysics*, **263**, 235–249.

Horváth, F. (1993) Towards a mechanical model for the formation of the Pannonian basin. *Tectonophysics*, **225**, 333–357.

Horváth, F. & Cloetingh, S. (1996) Stress-induced late-stage subsidence anomalies in the Pannonian basin. *Tectonophysics*, **266**, 287–300.

Jipa, D. (1997) Late Neogene-Quaternary evolution of Dacian basin (Romania). An analysis of sediment thickness patterns. *Geo-Eco-Marina*, **2**, 128–134.

Johnson, D.D. & Beaumont, C. (1995) Preliminary results from a planform kinematic model of orogen evolution, surface processes and the development of clastic foreland basin stratigraphy. In: *Stratigraphic Evolution of Foreland Basins. Special Publication of the Society of Econmics, Paleontology, and Mineralogy* pp 3–24. Society for sedimentary geology, Tulsa, Oklahoma.

Jones, P.B. (1996) Triangle zone geometry, terminology and kinematics. *Bull. Can. Petrol. Geol.*, **44**(2), 139–152.

Knapp, J.H., Knapp, C.C., Răileanu, V., Matenco, L., Mocanu, V. & Dinu, C. (2005) Crustal constraints on the origin of mantle seismicity in the Vrancea Zone, Romania: the case for active continental lithospheric delamination. *Tectonophysics*, **410**, 311–323.

Kovač, M., Nagymarosy, A., Oszczypko, N., Slaczka, A., Csontos, L., Marunteanu, M., Matenco, L. & Marton, E. (1999) Palinspastic reconstruction of the Carpathian-Pannonian region during the Miocene. In: *Geodynamic development of the Western Carpathians* (Ed. by M. Rakus), pp. 189–218. Dionyz Stur, Bratislava.

Krzywiec, P. (2001) Contrasting tectonic and sedimentary history of the central and eastern parts of the Polish Carpathian

foredeep basin – results of seismic data interpretation. *Mar. Petrol. Geol.*, **18**, 13–38.

Leever, K.A., Bertotti, G., Zoetemeijer, R., Matenco, L. & Cloetingh, S. (2006) The effects of a lithospheric strength transition on foredeep evolution: implications for the east Carpathian Foredeep. *Tectonophysics*, **421**(3–4), 251–267.

Marinescu, F., Ghenea, C. & Papaianopol, I. (1981) *Stratigraphy of the Neogene and the Pleistocene Boundary. Guide to Excursion A6, Carpatho-Balkan Geological Association XII Congress. Guidebook Series*. Institute of Geology and Geophysics, Bucharest.

Marinescu, F. & Papaianopol, I. (1995) La Depression de Transylvanie; le bassin Brasov-Baraolt. In: *Chronostratigraphie und Neostratotypen. Neogen der Zentrale Paratethys. Band IX, Dacien* (Ed. by F. Marinescu & I. Papaianopol), pp. 82–83. Editura Academiei Romane, Bucharest.

Matenco, L. & Bertotti, G. (2000) Tertiary tectonic evolution of the external East Carpathians (Romania). *Tectonophysics*, **316**, 255–286.

Matenco, L., Bertotti, G., Cloetingh, S. & Dinu, C. (2003) Subsidence analysis and tectonic evolution of the external Carpathian–Moesian platform region during Tertiary times. *Sediment. Geol.*, **156**, 71–94.

Matenco, L., Bertotti, G., Cloetingh, S., Marin, M., Schmid, S., Tărăpoancă, M. & Dinu, C. Coeval Pliocene - Quaternary differential vertical and horizontal movements in the SE Carpathians foreland: crustal versus lithospheric folding. *Tectonics*, in press.

Merten, S., Andriessen, P.A.M., Juez-Larré, J., Bertotti, G. & Dunai, T.J. (2005) Dating the exhumation of the Romanian carpathians: first results from Apatite (U–Th)/He Thermochronology. *Geophys. Res. Abst.*, **7**, 08138.

Morley, C.K. (1996) Models for relative motion of crustal blocks within the Carpathian region, based on restorations of the outer Carpathian thrust sheets. *Tectonics*, **15**, 885–904.

Mrazec, L. (1907) Despre cute au simbure de shapungere (On folds with piercing cores). *Soc. Stute Bull. Romania*, **16**, 6–8.

Necea, D., Fielitz, W. & Matenco, L. (2005) Late Pliocene–Quaternary large scale differential motions in the frontal part of the SE Carpathians: insights from tectonic geomorphology. *Tectonophysics*, **410**, 137–156.

Olteanu, R. (2003) The last representatives of the 'Pannonian' realm (Ostracoda, Crustacea). In: *Chronostratigraphie und Neostratotypen. Neogen der Zentrale Paratethys. Band X, Romanien* (Ed. by I. Papaianopol, F. Marinescu, N. Krstic & R. Macalet), pp. 350–375. Editura Academiei Romane, Bucharest.

Oncescu, M.C. & Bonjer, K.P. (1997) A note on the depth recurrence and strain release of large Vrancea earthquakes. *Tectonophysics*, **272**, 291–302.

Panea, I., Stephenson, R., Knapp, C.C., Mocanu, V., Drijkoningen, G., Matenco, L., Knapp, J. & Prodehl, K. (2005) Near-vertical seismic reflection image using a novel acquisition technique across the Vrancea Zone and Foscani Basin, south-eastern Carpathians (Romania). *Tectonophysics*, **410**, 293–309.

Popescu, M.N. & Drăgoescu, I. (1986) The new map of recent vertical crustal movements in Romania, scale 1 : 1,000,000. *Rev. Roum. Geol. Geophys. Geogr. Ser. Geophys.*, **30**, 31–10.

Răbăgia, T. & Matenco, L. (1999) Tertiary tectonic and sedimentological evolution of the South Carpathians foredeep: tectonic versus eustatic control. *Mar. Petrol. Geol.*, **16**(7), 719–740.

Rabus, B., Eineder, M., Roth, A. & Bamler, R. (2003) The Shuttle radar topography mission – new class of digital elevation models aquired by spaceborne radar. *Photogr. Rem. Sensing.*, **57**, 241–262.

Rădulescu, D.P., Cornea, I., Săndulescu, M., Constantinescu, P., Rădulescu, F. & Pompilian, A. (1976) Structure de la crôute terrestre en Roumanie. Essai d'interprétation des études séismiques profondes. *Ann. Inst. Geol. Geofiz.*, **50**, 5–36.

Radulian, M., Mândrescu, N., Panza, G.F., Popescu, E. & Utale, A. (2000) Characterization of seismogenic zones of Romania. In: *Seismic Hazards of the Circum-Pannonian Region. Pure and Applied Geophysics* (Ed. by G. Panza, M. Radulian, C. Trifu & F. Ioan), pp. 55–77. Birkhäuser Verlag, Basel.

RÖGL, F. (1999) Mediteranean and Paratethys. Facts and hypotheses of an Oligocene to Miocene paleogeography. *Geol. Carpath.*, **50**, 339–349.

Roure, F., Roca, E. & Sassi, W. (1993) The Neogene evolution of the outer Carpathian flysch units (Poland, Ukraine and Romania); kinematics of a foreland/ fold-and-thrust belt system. *Sediment. Geol.*, **86**, 177–201.

Royden, L.H. (1988) Late Cenozoic tectonics of the Pannonian Basin system. In: *The Pannonian Basin, a Study in Basin Evolution* (Ed. by L.H. Royden & F. Horvath), *AAPG Memoir*, **45**, 27–48.

Royden, L.H. (1993) The tectonic expression of slab pull at continental convergent boundaries. *Tectonics*, **12**, 303–325.

Royden, L.H. & Karner, G.D. (1984) Flexure of lithosphere beneath Apennine and Carpathian Foredeep Basins: evidence for an insufficient topographic load. *AAPG Bull.*, **68**(6), 704–712.

Ruszkiczay-Rüdiger, Z., Dunai, T.J., Bada, G., Fodor, L. & Horváth, E. (2005) Middle to late Pleistocene uplift rate of the Hungarian Mountain Range at the Danube Bend, (Pannonian Basin) using in situ produced 3He. *Tectonophysics*, **410**, 173–187.

Sanders, C., Andriessen, P. & Cloetingh, S. (1999) Life cycle of the East Carpathian Orogen: erosion history of a doubly vergent critical wedge assessed by fission track thermochronology. *J. Geophys. Res.*, **104**, 29095–29112.

Săndulescu, M. (1984) *Geotectonica României (Translated Title: GeoTectonics of Romania)* (Ed. Tehnică, Bucharest, 450pp.

Săndulescu, M. (1988) Cenozoic tectonic history of the carpathians. In: *The Pannonian Basin, a Study in Basin Evolution* (Ed. by L.H. Royden & F. Horvath), *AAPG Memoir*, **45**, 17–25.

Schmid, S.M., Fugenschuh, B., Matenco, L., Schuster, R., Tischler, M. & Ustaszewski, K. The Alps-Carpathians-Dinarides-connection: a compilation of tectonic units. *Eclogae Geol. Herv.*, in press.

Schlunegger, F. & Simpson, G. (2002) Possible erosional control on lateral growth of the European Central Alps. *Geology*, **30**, 907–910.

Seghedi, A. (2001) The North Dobrogea orogenic belt (Romania); a review. In: *Peri-Tethys Memoir 6; Peri-Tethyan rifti/ Wrench Basins and Passive Margins* (Ed. by P.A. Ziegler, W. Cavazza, A.F. Robertson & S. Crasquin-Soleau), *Memoires Museum Nat.Histoire Nature.*, **186**, 237–257.

Sperner, B., Lorenz, F., Bonjer, K., Hettel, S., Muller, B. & Wenzel, F. (2001) Slab break-off – abrupt cut or gradual detachment? New insights from the Vrancea Region (SE Carpathians, Romania). *Terra Nova*, **13**, 172–179.

Spratt, D.A. & Lawton, D.C. (1996) Variation in detachment levels, ramp angles and wedge geometries along the Alberta thrust front. *Bull. Can. Petrol. Geol.*, **44**(2), 313–323.

Ştefănescu, M., Dicea, O. & Tari, G. (2000) Influence of extension and compression on salt diapirism in its type area, East Carpathians Bend area, Romania. In: *Salt, Shale and Igneous Diapirs in and Around Europe* (Ed. by B.C. Vendeville, Y. Mart & J.L. Vigneresse), *Geol. Soc. Spec. Publ. London,* **174**, 131–147.

Suppe, J. (1983) Geometry and kinematics of fault-bend folding. *Am. J. Sci.*, **283**, 684–721.

Tărăpoancă, M. (2004). Architecture, 3D geometry and tectonic evolution of the Carpathians foreland basin. PhD Thesis, Vrije Universiteit, Amsterdam, 119pp.

Tărăpoancă, M., Bertotti, G., Matenco, L., Dinu, C. & Cloetingh, S. (2003) Architecture of the Focşani depression: a 13 km deep basin in the Carpathians bend zone (Romania). *Tectonics*, **22**(6), 1074, doi:10.1029/2002TC001486.

Thamó-Bozsó, E., Kercsmár, Z. & Nádor, A. (2002) Tectonic control on changes in sediment supply: quaternary alluvial system, Körös sub-basin, SE Hungary. In: *Sediment Flux to Basins: Causes, Controls and Consequences* (Ed. by S.J. Jones & L.E. Frostick), *Geol. Soc. Spec. Pub.London*, **191**, 37–53.

Twiss, R.J. & Moores, E.M. (1992) *Struct. Geol.*. Freeman Scientific, New York, 531pp.

Van der Hoeven, A.G.A., Mocanu, V., Spakman, W., Nutto, M., Nuckelt, L., Matenco, L., Munteanu, L., Marcu, C. & Ambrosius, B.A.C. (2005) Observation of present-day tectonic motions in the south-eastern Carpathians: geodetic results of the ISES/CRC-461 GPS measurements. *Earth Planett. Sci. Lett.*, **239**, 177–184.

Vasiliev, I., Krijgsman, W., Langereis, C.G., Panaiotu, C.E., Matenco, L. & Bertotti, G. (2004) Magnetostratigraphic dating and astronomical forcing of the Mio-Pliocene sedimentary sequences of the Focşani basin (Eastern Paratethys – Romania). *Earth Planet. Sci. Lett*, **227**, 231–247.

Vasiliev, I., Krijgsman, W., Stoica, M. & Langereis, C.G. (2005) Mio-Pliocene magnetostratigraphy in the southern Carpathian foredeep and Mediterranean–Paratethys correlations. *Terra Nova*, **17**, 376–384.

Visarion, M., Săndulescu, M., Stănica, D. & Veliciu, S. (1988) Contributions á la connaissance de la structure profonde de la plate-forme Moésienne en Roumanie. *St. Tehn. Econ. Geofiz.*, **15**, 68–92.

Weidle, C., Widiyantoro, S. & Calixto Working Group (2005) Improving depth resolution of teleseismic tomography by simultaneous inversion of teleseismic and global P-wave traveltime data – application to the Vrancea region in Southeastern Europe. *Geophys. J. Int*, **162**, 811–823.

Wenzel, F., Lorenz, F., Sperner, B. & Oncescu, M.C. (1999) Seismotectonics of the Romanian Vrancea area. In: *Vrancea Earthquakes: Tectonics, Hazard and Risk Mitigation* (Ed. by F. Wenzel, D. Lungu & O. Novak) Kluwer Academic Publishers, Dordrecht, Netherlands, pp. 15–26.

Wortel, M.J.R. & Spakman, W. (2000) Subduction and Slab Detachment in the Mediteranean–Carpathian Region. *Science*, **290**, 1910–1917.

Zweigel, P., Ratschbacher, L. & Frisch, W. (1998) Kinematics of an arcuate fold-thrust belt: the southern East Carpathians (Romania). *Tectonophysics*, **297**, 177–207.

